

MICROCOPY RESOLUTION TEST CHART
NATIONAL BUREAU OF STANDARDS-1963-A

ATC Report No. R-91000/9CR-66
Contract No. N00019-79-C-0136

LETT II

2
SR

AD A090331

Turbulence Modeling for Application to V/STOL Propulsion Induced Effects - Two Dimensional Formulation

A. H. Ybarra

Vought Corporation Advanced Technology Center
Dallas, Texas 75266

DTIC
ELE
OCT 14 1980
S A

December 1979

Final Report for Period January - October 1979

Approved for public release, distribution unlimited

Prepared for:

Department of the Navy
Naval Air Systems Command
Washington, D. C. 20361

DDC FILE COPY



VOUGHT CORPORATION
Advanced Technology Center

80 10 6 148

Unclassified

SECURITY CLASSIFICATION OF THIS PAGE (When Data Entered)

REPORT DOCUMENTATION PAGE		READ INSTRUCTIONS BEFORE COMPLETING FORM
1. REPORT NUMBER	2. GOVT ACCESSION NO. AD-A090 331	3. RECIPIENT'S CATALOG NUMBER
4. TITLE (and Subtitle) Turbulence Modeling for Application to V/STOL Propulsion Induced Effects - Two Dimensional Formulation,		5. TYPE OF REPORT & PERIOD COVERED Final (Jan-Oct, 1979)
7. AUTHOR(s) Andres H. Ybarra		6. PERFORMING ORG. REPORT NUMBER R-91000/9CRL-66
9. PERFORMING ORGANIZATION NAME AND ADDRESS Vought Corporation Advanced Technology Center P. O. Box 226144 Dallas, Texas 75266		8. CONTRACT OR GRANT NUMBER(s) N00019-79-C-0136
11. CONTROLLING OFFICE NAME AND ADDRESS Naval Air Systems Command NAIR 320D Washington, D. C. 20361		10. PROGRAM ELEMENT, PROJECT, TASK AREA & WORK UNIT NUMBERS
14. MONITORING AGENCY NAME & ADDRESS (if different from Controlling Office) Naval Air Systems Command NAIR 320D Washington, D. C. 20361		12. REPORT DATE 15 November 1979
		13. NUMBER OF PAGES 60
		15. SECURITY CLASS. (of this report) Unclassified
		15a. DECLASSIFICATION/DOWNGRADING SCHEDULE
16. DISTRIBUTION STATEMENT (of this Report) Approved for public release: Distribution unlimited		
17. DISTRIBUTION STATEMENT (of the abstract entered in Block 20, if different from Report)		
18. SUPPLEMENTARY NOTES		
19. KEY WORDS (Continue on reverse side if necessary and identify by block number) Turbulence Model Lift Jet Entrainment Boundary Layer Flow V/STOL		
20. ABSTRACT (Continue on reverse side if necessary and identify by block number) Feasibility is established for the use of a statistical vortex model of turbulence to characterize shear flows associated with mixing and entrainment. The model is an extension of an approach used successfully for prediction of inlet flow maximum distortion levels. Analytically it forms the closure required for the governing Reynolds and kinetic energy turbulent flow equations. Applicability of the model to shear flows is validated by focusing on fully developed turbulent flow in a two-dimensional		

DD FORM 1 JAN 73 1473

EDITION OF 1 NOV 68 IS OBSOLETE
S/N 0102-014-6601

Unclassified
SECURITY CLASSIFICATION OF THIS PAGE (When Data Entered)

Unclassified

SECURITY CLASSIFICATION OF THIS PAGE(When Data Entered)

channel. The solutions completely characterize the flow with a single distributive set of vortex (or eddy) properties. This includes the mean velocity profiles, cross correlation (Reynolds) stress terms, root-mean-square levels of the axial and lateral velocity perturbations, and energy production, diffusion, and dissipation terms. Comparisons with an extensive channel data base verify the characterization. In addition, the solutions provide the framework for coupling the analytics with experimental boundary (or initial) conditions to define scaling relations. The studies indicate that a definite variation in turbulence eddy properties exists across the channel. These variations can be determined from measurements of the flow field unsteady pressure fluctuations. The results are applicable to turbulent flow boundary layers and flow mixing problems in general, and ultimately to aircraft propulsion induced effects (e.g., VSTOL) where jet mixing and entrainment dominate the flight/model scaling and simulation requirements.

Unclassified

SECURITY CLASSIFICATION OF THIS PAGE(When Data Entered)

SUMMARY

The specific objective of this program was to establish the feasibility of developing an analytical model for solving the Reynolds Equations of Motion for fully developed two-dimensional channel turbulent flow. During the course of these studies, feasibility of using the Turbulent Flow Models to provide the closure necessary to solve the Reynolds Equation has been demonstrated.

Closed form solutions have been obtained, by use of the Turbulent Flow Model, for the mean velocity profile, the cross correlation (Reynolds) stress term and for the root-mean-square levels of the axial and lateral velocity perturbations. These solutions compare very well with measurements recorded by John Laufer in 1951. The Turbulent Flow Model was also used to obtain solutions of the three terms of the Turbulent Kinetic Energy Equation - Production, diffusion and dissipation terms. These solutions also agree well with the measured data.

The studies indicate that a definite variation in turbulence eddy properties exists across the channel. These variations can be determined from measurements of the flow field unsteady pressure fluctuations.

A procedure for extending the current procedures to the case of axisymmetric flow is included.

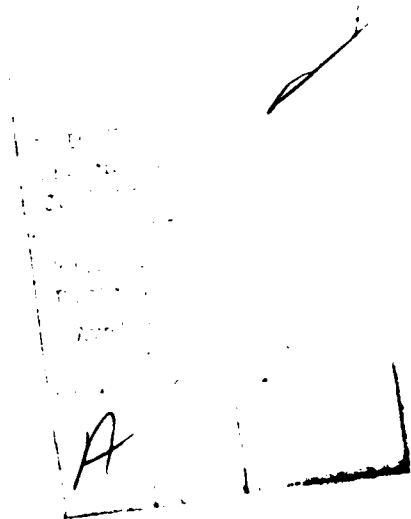


TABLE OF CONTENTS

	<u>Page</u>
SUMMARY	iii
TABLE OF CONTENTS	iv
LIST OF FIGURES	v
LIST OF TABLES	vi
1.0 INTRODUCTION	1
2.0 DISCUSSION	2
2.1 Turbulent Flow Model	3
2.2 Unsteady Velocity Correlations	12
2.3 Distributions of Vortex Properties	25
2.4 Effects of Boundary Conditions	29
2.5 Data/Analysis Comparisons	34
2.6 Analysis for Axisymmetric Flow and Jet Mixing	50
3.0 CONCLUSIONS AND RECOMMENDATIONS	51
REFERENCES	52
NOMENCLATURE	53

LIST OF FIGURES

	<u>Page</u>
1. Turbulent Flow in a Two-Dimensional Open Channel after Photographs by Prandtl.	4
2. Plane Mixing Between Two Streams with Velocities U_1 and U_2 , Densities ρ_1 and ρ_2	4
3. Mixing Layer Between Helium (Upper) and Nitrogen Streams, $U_2/U_1 = 0.38$, After Roshko.	5
4. Mixing Layer Between Nitrogen (Upper) and a Helium-Orgon Mixture of Same Density, After Roshko	5
5. Vortex Model Flow Field	6
6. Hypothesized Turbulent Flow Composed of Random Vortices	6
7. Statistical Properties of the Turbulent Flow Model.	11
8. Mean Velocity Profiles Computed Using Uniform Vortex Properties.	16
9. Vortex Strength Distributions	27
10. Vortex Size Distributions	28
11. Fully Developed 2-D Channel Incompressible Laminar Flow	32
12. Fully Developed 2-D Channel Incompressible Turbulent Flow	33
13. Summary of Turbulent Flow Data in 2-D Channel, Reference (2).	35
14. Turbulent Energy Balance Data, Reference (2).	36
15. Mean Velocity Profiles Computed Using Arbitrary Vortex Distributions.	38
16. Comparisons of Data and Predictions with Distribution A2V4.	39
17. Comparisons of Data and Predictions with Distributions A3V1	40
18. Vortex Strength and Size Distributions.	41
19. Comparisons of Data and Prediction with Distribution V29B	44
20. Comparisons of Data and Prediction with Distribution V34.	45
21. Comparisons of Data and Prediction with Distribution V36.	46
22. Comparisons of Data and Prediction with Distribution V42.	47
23. Comparisons of Data and Prediction with Distribution V47.	48
24. Comparisons of Data and Prediction with Distribution V57.	49

LIST OF TABLES

	<u>Page</u>
I. Velocity and Perturbations Due to Vortex in 2-D Duct	8
II. Velocity Components from Vortex Model	13
III. Number of Vortices in 2-D Duct	20
IV. Time Average Velocity Induced by Vortices	21
V. Velocity Correlation Terms	22
VI. TKE Dissipation and Diffusive Terms	24

1.0 INTRODUCTION

The large mass flows and high degree of integration required of V/STOL type propulsion systems affect the local flow fields around the aircraft. These propulsion induced effects can substantially alter the performance of the aircraft in V/STOL operations. Forces resulting from suckdown and jet fountain can modify the lift and pitch and roll moments. Such forces can be appreciable as measured in scale model test programs. Similarly, exhaust gas reingestion degrades thrust available. Consequently, it is important to properly model the propulsive jet when testing with scale models. Different results have been found when using different jet sources such as model fan, compressed air jet, or ejector type propulsion simulators. Apparently, different jets which are similar in velocity and diameter create different downwash and ground jet flow fields with differing amounts of entrainment and different airframe induced forces and moments. From such results, past V/STOL aircraft performance has not been predicted with acceptable accuracy even though extensive controlled model data was used. Improved jet entrainment simulation and understanding of model jet scaling is required to overcome this type of V/STOL program hazard.

Jet entrainment is dependent on the jet velocity profile and turbulence level which at present are not accounted for in model testing or in mathematical models of jet entrainment and mixing. The ultimate goal of this program is to develop a model that will account for all the major parameters in the mixing process, such that jet entrainment can be modeled.

The objective of this program was to establish the feasibility of solving the Reynolds Equations analytically through application of the statistical fluid dynamic model of turbulence to channel flow. This fluid dynamic model has been successfully applied to the turbulent flow in inlet systems and will provide the link between the statistical properties of turbulence and the steady state velocity gradients. Results will enable prediction of the steady state velocity profile and Reynolds stresses throughout the channel flow field.

The technique will enable an analytical solution of the Reynolds Equations of Motion without recourse to empirical constants such as mixing length or eddy viscosity coefficient. The results are applicable to turbulent flow boundary layers and flow mixing problems in general, and ultimately to aircraft propulsion induced effects.

2.0 DISCUSSION

The ultimate goal of this program is the development of an analytical model for the simulation of jet entrainment and mixing. Jet entrainment can be characterized as a highly complex case of turbulent free shear flow. The case of fully developed turbulent flow in a two-dimensional channel is the simplest flow problem, and therefore was chosen as the model for the present feasibility study. A previously developed turbulence model¹ was used to obtain closure of the turbulent flow equations without recourse to strictly empirical constants. The model has physical basis in the coherent vortex approach.

A discussion of the elements investigated during the feasibility study are presented in this section. A review of the turbulent flow model is first presented. This model is developed using fundamental laws of fluid mechanics and statistical mathematics and is based on a series of eddies of random size and strength convected by the local flow. The elementary results of this turbulence model are the unsteady velocity perturbations. These perturbations are then combined to obtain the mean and root-mean-square parameters that define the turbulent flow field. The variations of these parameters depend on the statistical behavior of the turbulence model random variables.

These random variables (eddy size, strength, location, spin direction, etc.) are in turn dependent on the actual turbulent flow field. The second part of the study presented in this section shows how turbulence flow measurements in terms of the fluctuating total pressure root-mean-square values define the distribution of vortex properties. Since these measurements were not available, representative distributions were used and refined until good correlation with test data was obtained.

Derivation of the unsteady velocity correlation terms is presented. These terms include the axial and lateral velocity components ($\overline{u'^2}$ and $\overline{v'^2}$) and the cross correlation terms ($\overline{u'v'}$). Also, terms in the Turbulent Kinetic Energy Equation are presented.

The form of the Reynolds Equation of Motion applicable to the two-dimensional channel flow is presented. A discussion of the boundary conditions and their effects is also included.

Comparisons are made between the various flow parameters as measured by Laufer and reported in Reference 2 and the corresponding predictions made by the current analytical work. These predictions include all the elements of the study.

An outline of the steps for extending the analytical method to the case of axisymmetric flow is presented. This is the second step in developing the analytical model for the simulation of jet entrainment and mixing.

2.1 TURBULENT FLOW MODEL

An analytical model of turbulent inlet flow was developed and reported in Reference 1. This model accounts for the fundamental fact that turbulence is random in character, and consequently that a statistical analysis of the flow is an essential requirement. To model this random inlet turbulence, it was hypothesized that measured pressure fluctuations result from a random distribution of discrete vortices being convected downstream by the mean flow. Tangential velocity and local pressure gradients associated with each vortex, when superimposed on the mean flow, produce these measured pressure fluctuations. Fundamental fluid mechanics is used to describe the characteristics of discrete vortices and their superposition on the mean flow, while standard statistical methods are used to generate the random nature of the flow field. By use of this model, the size and strength of the momentary low pressure regions are defined.

A physical model of turbulent inlet flow is developed by consideration of the nature of turbulence. This model is then formulated mathematically by use of fundamental laws governing fluid flow and by application of statistical techniques to the random character of the flow.

Physical Description of Turbulent Flow Model

Fully developed turbulent flow in a channel will have a symmetrical velocity profile as indicated in Figure 1(a). By using appropriate flow visualization techniques, a time exposure taken of this flow will show streamlines as sketched in Figure 1(b). Photographs taken by Prandtl,³ with the camera moving at speeds approaching that of the fluid, show vortices being convected along with the local mean flow as in Figure 1(c) and (d). Therefore, the concept of a straight streamline is only true on a time averaged basis. The actual fluid particle experiences a non-uniform motion, which is dependent on the turbulence level.

Roshko discusses the case of the turbulent mixing layer in Reference 4. Figure 2, which has been taken from Reference 4, is a schematic of this type of flow in which the uniform streams on either side of the mixing layer are characterized by their velocities, U_1 and U_2 , etc. Shadow pictures of the flow revealed the presence of well defined large structures (Figures 3 and 4) which have the appearance of breaking waves or rollers or vortices, superimposed on a background of finer scaled turbulence.

It is hypothesized that turbulent channel flow is composed of vortices of various size and strength that are convected downstream at the local velocity. This hypothesis is fundamental to the proposed analysis and is shown schematically in Figure 5. Such vortices created by the steady state velocity profile (U, V) produce unsteady velocity components (u, v) as measured in the coordinate system fixed to the channel walls. The flowfield about each vortex, however, is steady in a coordinate system fixed to the vortex, i.e., moving at the local velocity. Consequently, the vortex flowfield can be analyzed using steady state flow

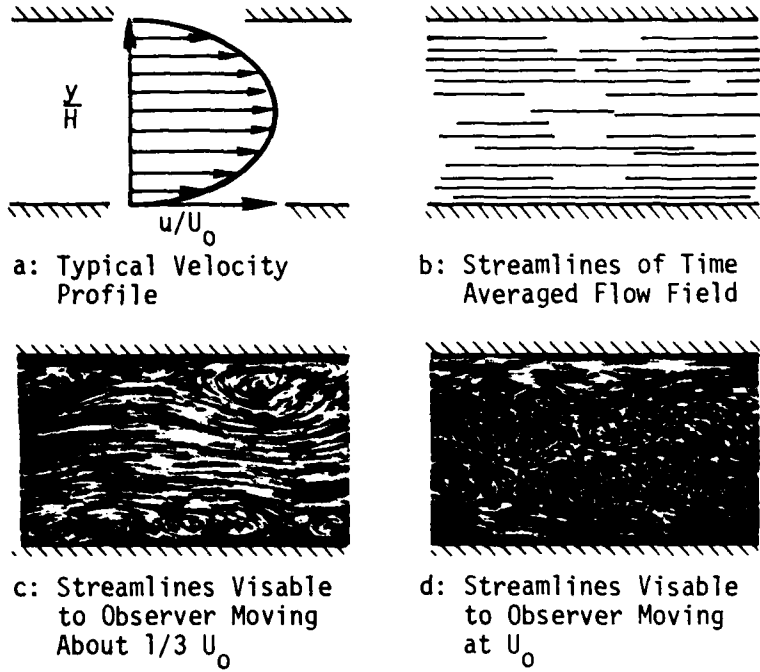


Figure 1. Turbulent Flow in a Two-Dimensional Open Channel after Photographs by Prandtl

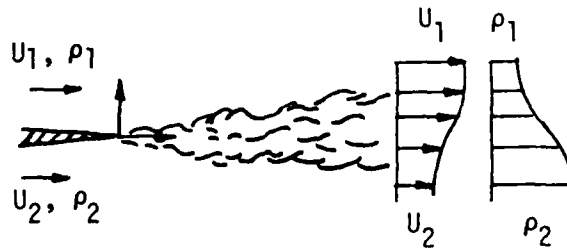


Figure 2. Plane Mixing between Two Streams with Velocities U_1 and U_2 , Densities ρ_1 and ρ_2

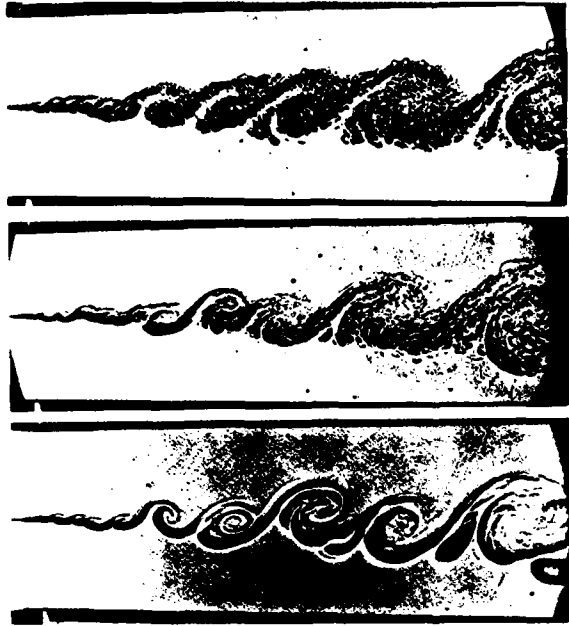


Figure 3. Mixing Layer Between Helium (upper) and Nitrogen Streams, $U_2/U_1 = 0.38$, After Roshko

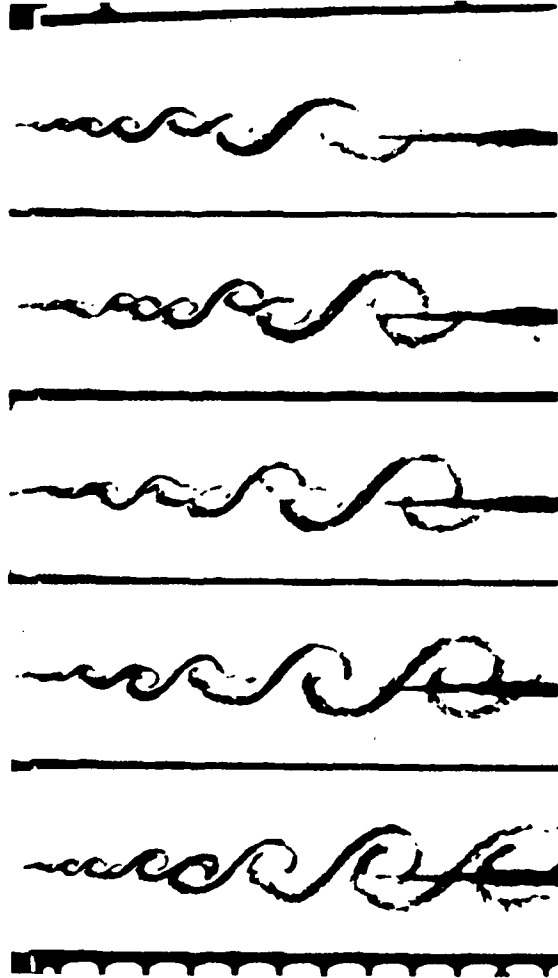
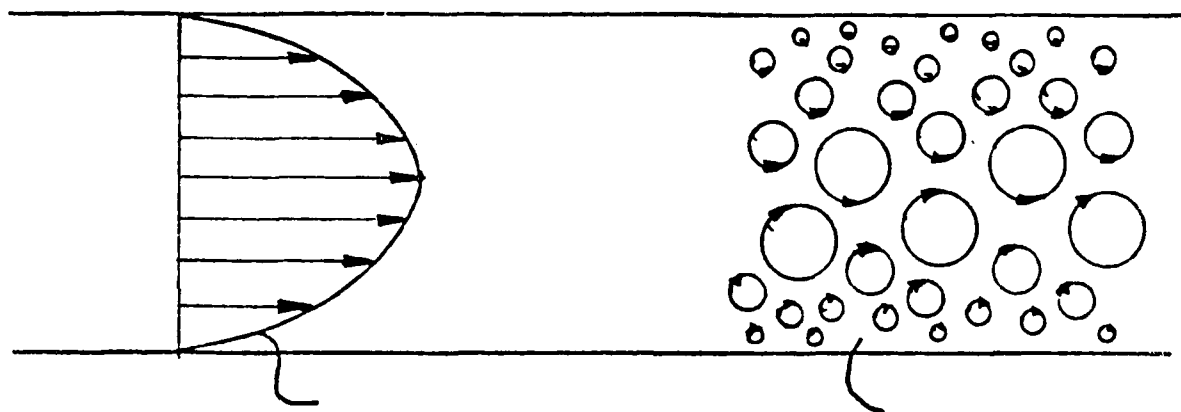


Figure 4. Mixing Layer Between Nitrogen (upper) and a Helium-Argon Mixture of Same Density, After Roshko

VELOCITY PROFILE

VORTEX DISTRIBUTION



Each vortex is described by its size, a
 strength, $V_{\theta m}$
 location, Y
 rotation, ± 1

Figure 5. Vortex Model Flow Field

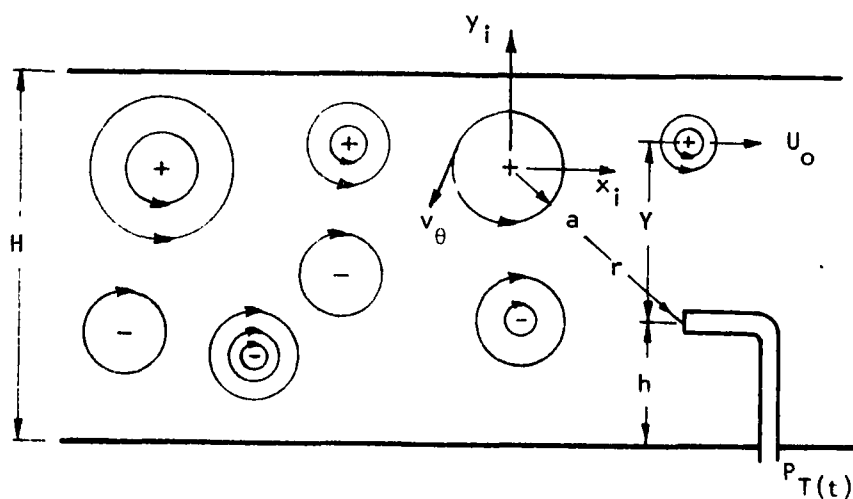


Figure 6. Hypothesized Turbulent Flow
 Composed of Random Vortices

equations. The velocity fluctuations are generated from superposition of the vortex flowfield on the local flow. The turbulent nature of the flow results from a distribution of these vortices having random size, strength, location, and orientation. The turbulence terms u'^2 , v'^2 , $u'v'$ can be determined by application of statistical methods to the combined flowfield definition.

Isolated Vortex Flowfield

As the first step in the mathematical development of the flow model, the two-dimensional incompressible Navier-Stokes Equations of Motion were solved to derive the flow properties of an isolated vortex with a viscous core and inviscid, potential flow at large radii. Definition of the variables that comprise the flow model are illustrated in Figure 6. The normalized velocity field associated with this vortex for a coordinate system located at the center of the vortex is given by Equation (1).

$$v_{\theta} / v_{\theta m} = n(r/a) e^{-1/2[(r/a)^2 - 1]} \quad (1)$$

where v_{θ} is the tangential velocity and "a" the radius at which the tangential velocity is a maximum. The parameters "a" and $v_{\theta m}$, are used to characterize the size and strength of the vortex, respectively, with "a" being considered the radius of the vortex core. The associated static pressure profile through the vortex is given in Equation (2).

$$P - P_0 = - \frac{\rho}{2} v_{\theta m} e^{-[(r/a)^2 - 1]} \quad (2)$$

where P_0 is the pressure at $r/a \gg 1$, and ρ is the density.

The vortex tangential velocity, Equation (1), can be expressed in terms of the horizontal (axial) and vertical (lateral) velocity components. Since the radius to a point (x,y) in the flow field is $r^2 = x^2 + y^2$, the velocity components are:

$$u = -nv_{\theta m} (y/a) e^{-\frac{1}{2}[(x/a)^2 + (y/a)^2 - 1]} \quad (3a)$$

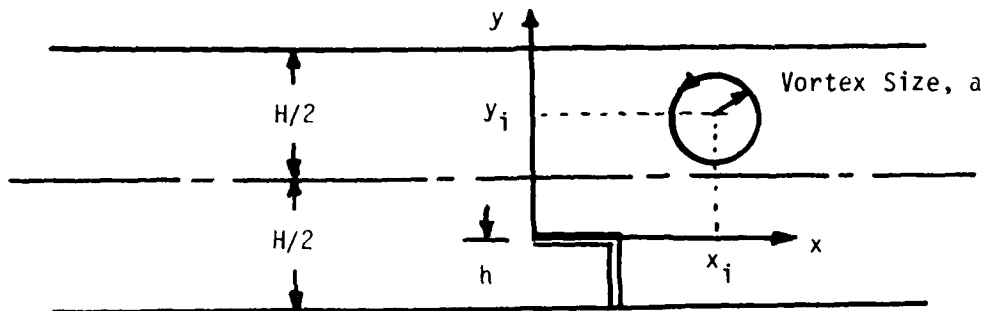
$$v = nv_{\theta m} (x/a) e^{-\frac{1}{2}[(x/a)^2 + (y/a)^2 - 1]} \quad (3b)$$

Flowfield Due to Single Vortex

To determine the effects of this isolated vortex on the flowfield "fixed" to the channel, a coordinate transformation is required. Consider the sketch in Table I. The point of interest in the flowfield is the "total pressure probe" face. It is desired to define the flowfield characteristics at the probe

TABLE I

VELOCITY AND PRESSURE PERTURBATIONS DUE TO VORTEX IN 2-D DUCT



- | | | | |
|----------------|--|---|--|
| H | - Duct Height | v | - Perturbation velocity in y direction |
| h | - Probe location | u | - Perturbation velocity in x direction |
| x _i | - x location of vortex "i" | U | - Velocity in x direction |
| y _i | - y location of vortex "i" | n | - Index of rotation, counterclockwise = +1, clockwise = -1 |
| a | - Vortex size (radius) | | |
| v _m | - Vortex tangential velocity at radius a | | |

The following velocities are due to a vortex as described in above sketch and were developed in Reference 1.

$$u(t) = \pi v_{om} \left(\frac{y}{a}\right) e^{-\frac{1}{2} \left[\left(\frac{ut}{a}\right)^2 + \left(\frac{y}{a}\right)^2 - 1 \right]} \quad (I-1)$$

$$v(t) = -n v_{om} \left(\frac{ut}{a}\right) e^{-\frac{1}{2} \left[\left(\frac{ut}{a}\right)^2 + \left(\frac{y}{a}\right)^2 - 1 \right]} \quad (I-2)$$

$$p(t) = -\frac{1}{2} \rho v_{om}^2 e^{-\frac{1}{2} \left[\left(\frac{ut}{a}\right)^2 + \left(\frac{y}{a}\right)^2 - 1 \right]} \quad (I-3)$$

due to the presence of a single vortex. At any instance of time the single vortex is located at some distance x_i, y_i from the probe. Since the vortex is convected by the local flow, its location in the x-direction can be expressed as

$$x_i = Ut$$

where the time $t = 0$ is taken as the instance when the vortex passes the probe station ($x = 0$). The resultant pressure and velocity perturbation equations are given in Table I.

The total pressure fluctuations due to the passage of a single vortex can be expressed in a similar manner. Total pressure is defined as the sum of the static and dynamic pressures. Using only the axial component of velocity, the total pressure as measured at the probe is

$$P_T = P + \frac{\rho}{2} (U_o + u)^2 = P + \frac{\rho}{2} (U_o^2 + 2U_o u + u^2) \quad (5)$$

The fluctuation in total pressure, normalized by velocity head, is dependent on the velocity fluctuations and is given by

$$\frac{\Delta P_T}{q_o} = \frac{P - P_o}{q_o} + \frac{2u}{U_o} + \left(\frac{u}{U_o}\right)^2 \quad (6)$$

This total pressure fluctuation is of interest because it will be used later to define the vortex properties (size and strength) mean distributions.

Statistical Description of Turbulent Flow

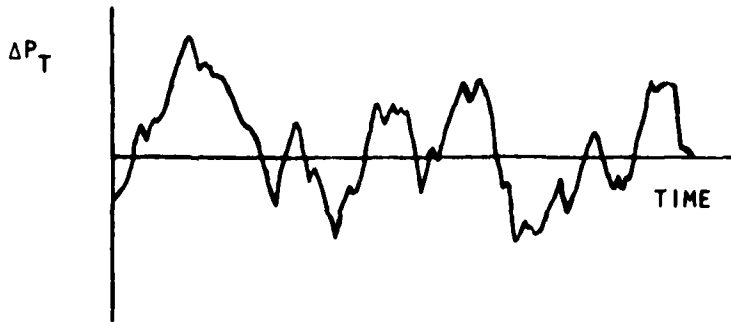
Turbulent fluid motion as defined by Hinze,⁵ is an irregular condition of flow in which various measurements of pressure, velocity, etc., show a random variation with time. This random motion is, however, amenable to description by the laws of probability and distinct average values.

The root mean square (RMS) level and power spectral density (PSD) function of total pressure fluctuations are two examples of average values that are commonly used. Since in this model of turbulence, low pressure regions are caused by vortices passing an arbitrary geometric station, it is necessary to relate the RMS level and PSD function to the characteristic properties of the vortices. These relationships are developed in Reference 1 and include: (1) the relationship of the root mean square level to the mean strength of the vortices, and (2) the relationship of the power spectral density function to the mean size of the vortices. The power spectra computed from the analysis are compared with that obtained from test data to provide verification of the turbulent flow model.

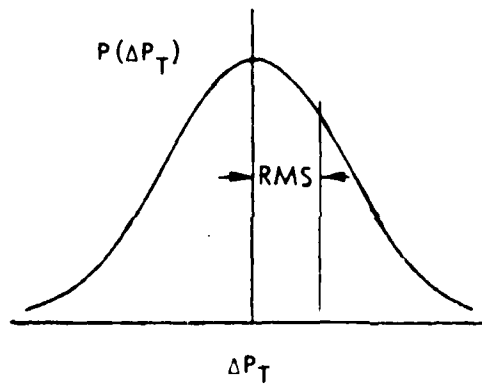
Typical statistical measurements for a single probe are shown in Figure 7. Figure 7(a) shows the time trace of the total pressure fluctuations which are random in nature - in the magnitude, duration, and direction of the pressure pulses. The time history can be expressed as a probability density function (histogram) of the pressure fluctuation as shown in Figure 7(b). Mathematically, the histogram is the autocorrelation function of the pressure pulse at the probe. The probability density function represents both the range of pressure fluctuations and the relative occurrence of each level. The time average is zero, hence steady state. The total pressure RMS level is the mean value of these pressure fluctuations. Transformation of this information from the time domain to the frequency domain yields the power spectral density function, Figure 7(c).

These two functions, Figure 7(b) and 7(c) define the vortex properties. The magnitude of the pressure fluctuation in Figure 7(a) depends directly on the vortex tangential velocity, Figure 6. The magnitude of the fluctuations determine the histograms' RMS level. Therefore, the RMS level is a direct measure of the vortex tangential velocity or strength. The duration of a pressure pulse in Figure 7(a) depends directly on the size of the vortex passing the probe location, Figure 6. The pressure pulse from a large vortex will have a greater duration than the pulse from a small vortex. These periods of pulse durations are expressed as frequency of occurrence in the frequency domain, the PSD function, Figure 7(c). The PSD curve represents the distribution of vortex sizes that pass the probe stations. Vortices of small size will appear at the higher frequencies and vortices of large size will appear at the lower frequencies. The PSD curve shape therefore, determines the average vortex size.

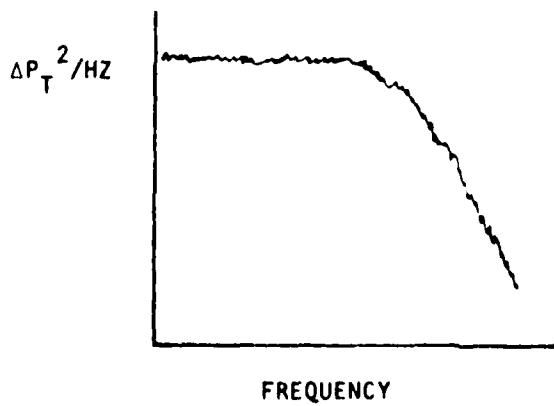
These two relationships can be used to determine the distribution of vortex size and strength at each point across the channel. Unsteady pressure data in these forms was not available for the present feasibility study, but could be obtained in a subsequent investigation.



(a) TIME TRACE OF ΔP_T



(b) HISTOGRAM OF ΔP_T



(c) POWER SPECTRUM OF ΔP_T

Figure 7. Statistical Properties of the Turbulent Flow Model

2.2 UNSTEADY VELOCITY CORRELATIONS

The Navier-Stokes Equations are considered valid for turbulent flow if actual velocities, etc., are used. Since the actual turbulent flow quantities are functions of time, the Navier-Stokes Equations for two-dimensional channel flow take the form:

$$U \frac{\partial U}{\partial x} + V \frac{\partial U}{\partial y} + \frac{\partial U}{\partial t} = \frac{1}{\rho} \left(\frac{\partial P}{\partial x} + \mu \nabla^2 U \right) \quad (7a)$$

$$U \frac{\partial V}{\partial x} + V \frac{\partial V}{\partial y} + \frac{\partial V}{\partial t} = \frac{1}{\rho} \left(\frac{\partial P}{\partial y} + \mu \nabla^2 V \right) \quad (7b)$$

The dependent variables can be replaced by the mean time average plus the fluctuation components. For instance, U and V are replaced by $\bar{U} + u$ and $\bar{V} + v$. The Navier-Stokes equations then take on the following form, the Reynolds Equations of Motion.

$$U \frac{\partial U}{\partial x} + V \frac{\partial U}{\partial y} = - \frac{1}{\rho} \frac{\partial P}{\partial x} + \nu \left(\frac{\partial^2 U}{\partial x^2} + \frac{\partial^2 U}{\partial y^2} \right) - \frac{\partial \overline{u^2}}{\partial x} - \frac{\partial \overline{uv}}{\partial y}$$

negligible in Turbulent Flow Reynolds Stress Terms

$$U \frac{\partial V}{\partial x} + V \frac{\partial V}{\partial y} = - \frac{1}{\rho} \frac{\partial P}{\partial y} + \nu \left(\frac{\partial^2 V}{\partial x^2} + \frac{\partial^2 V}{\partial y^2} \right) - \frac{\partial \overline{uv}}{\partial x} - \frac{\partial \overline{v^2}}{\partial y}$$

$$\text{where } U(t) = \bar{U} + u$$

$$V(t) = \bar{V} + v$$

The upper case symbols denote the time average (or steady state value) and the lower case symbols denote the fluctuation components. Reynolds stress terms are dependent on fluctuating components of the turbulent flow. The second term on the righthand side of the equations represent the laminar flow shear stress terms. Whereas, these terms are not identically zero, they are small compared to the turbulent shear stress term and therefore can be neglected.

Time averaged unsteady velocity components of the turbulent flow can be established from the turbulent flow model, as listed in Table II. The axial and lateral velocity components are first described for a single vortex. These are dependent on time (t) and on the vortex properties of size (a), strength (v_{em}), and spin direction (n). Unsteady velocity correlation terms are then found as the correlation term for a single vortex, multiplied by the total number of vortices per unit time (N) and weighted by the respective probabilities of all the random variables. These are shown in Table II in functional form.

2.2.1 Solution Procedures

Three methods for obtaining solutions of the unsteady velocity component integral equations in Table II are discussed. The first is the simplest and is based on using uniform vortex properties across the channel. The second method introduced is the most complex. It was developed in conjunction with the use of the Turbulent Kinetic Energy (TKE) Equation. The final approach is based on using vortex stability criteria as the basis for establishing the vortex flux (N).

TABLE II

VELOCITY COMPONENTS FROM VORTEX MODEL

$$\overline{u'^2} = N \iiint \int u(t) u(t) \mathcal{P}(Y) \mathcal{P}(n) \mathcal{P}(V_{em}) \mathcal{P}(a) dt da dV_{em} dn dY \quad (\text{II-1})$$

$$\overline{v'^2} = N \iiint \int v(t) v(t) \mathcal{P}(Y) \mathcal{P}(n) \mathcal{P}(V_{em}) \mathcal{P}(a) dt da dV_{em} dn dY \quad (\text{II-2})$$

$$\overline{u'v'} = N \iiint \int u(t) v(t) \mathcal{P}(Y) \mathcal{P}(n) \mathcal{P}(V_{em}) \mathcal{P}(a) dt da dV_{em} dn dY \quad (\text{II-3})$$

$$\bar{u} = N \iiint \int u(t) \mathcal{P}(Y) \mathcal{P}(n) \mathcal{P}(V_{em}) \mathcal{P}(a) dt da dV_{em} dn dY \quad (\text{II-4})$$

$$\bar{v} = N \iiint \int v(t) \mathcal{P}(Y) \mathcal{P}(n) \mathcal{P}(V_{em}) \mathcal{P}(a) dt da dV_{em} dn dY \quad (\text{II-5})$$

2.2.1.1 Uniform Properties

The simplest solution is obtained by assuming that the vortex properties are constant (uniform). For instance, the mean velocity profile for the 2-D channel flow can be found from the integral equation:

$$\bar{U} = N \int_a \int_x \int_v \int_t u(t) P(v_0) P(Y) P(a) dt dv_0 dY da \quad (8)$$

where, N is the eddy flux (number of vortices per unit time).

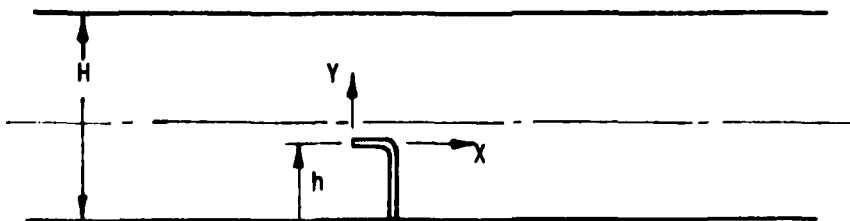
P() are the probability density functions for the vortex random properties. u(t) is defined by equation (1-1).

The multiple integral equation can be evaluated sequentially by integrating one variable at a time. The first variable is the time variable. The limits of integration are from $t = -\infty$ to $t = +\infty$. That is, the influence of each eddy is considered from a far distance upstream to a far distance downstream of the sensing element.

The second variable of integration is the eddy strength (v_0). This has been assumed to be constant across the channel. The minimum strength physically possible is zero. The maximum postulated strength in the eddy model is the local velocity U.

The eddy size is also assumed to be constant. The minimum size possible is zero and the maximum size permitted is the channel height H.

The eddy location and spin direction are treated in conjunction with one another. The eddy location probability density function is assumed to be uniform. All the eddies in each half of the channel are assumed to spin in the same direction. The mean velocity at a probe position is found by integrating equation (8) from lower wall to upper wall. Since all eddies below the centerline will rotate



clockwise, in this range the limits of integration are $-h$ to $H/2-h$. In the upper half of the channel, the eddies will spin counter-clockwise and the limits of integration are $H/2-h$ to $H-h$. The resultant integral solution is:

$$\frac{\bar{u}}{U_0} = \sqrt{\frac{e}{8}} \left(\frac{v_0}{U} \right) \left[2e^{-\frac{1}{2} \left(\frac{h}{a/H} \right)^2} - e^{-\frac{1}{2} \left(\frac{1-h/H}{a/H} \right)^2} - e^{-\frac{1}{2} \left(\frac{h/H}{a/H} \right)^2} \right] \quad (9)$$

Equation (9) was evaluated assuming different values of the eddy size a/H . The velocity profile was normalized so that the velocity is zero at the wall and maximum at centerline. The results are shown in Figure 8. These profiles resemble laminar flow profiles more than the turbulent profile represented by the test data of Laufer. The mismatch in profiles is due to the uniform distributions assumed for the vortex random properties.

2.2.1.2 Vortex Started Impulsively

All preceding work with the turbulent flow model assumed that the vortex properties remained constant during the time period of interest. That is, the flow field about each vortex was independent of time. In reality, the eddies that exist in the turbulent flow are changing in size and strength as they are convected downstream. Therefore, the more basic form of the flow field about a vortex started impulsively at time $t=0$ was used to describe the turbulent flow. Each such vortex would then be allowed to grow in size and decay in strength with time. However, the development led to a highly intractable integral form.

G. I. Taylor in 1918 gave the solution of a vortex flow field which satisfies the unsteady Navier-Stokes Equations and the proper boundary conditions. This solution represents a vortex formed instantaneously in undisturbed flow. The influence of this impulse begins to propagate outward at time $t=0$. The vortex flow field is defined by:

$$v_{\theta} = B \frac{r}{t^2} e^{-\frac{r^2}{4\nu t}} \quad (10)$$

where: v_{θ} = velocity in angular direction
 B = constant
 r = radius
 t = time
 ν = kinematic viscosity = μ/ρ

The radius (a) at which the velocity is maximum can be determined by setting the derivative $\partial v_{\theta} / \partial r$ equal to zero, or:

$$\frac{\partial v_{\theta}}{\partial r} = \frac{B}{t^2} e^{-\frac{r^2}{4\nu t}} - \frac{2Br^2}{4\nu t^3} e^{-\frac{r^2}{4\nu t}} = 0$$

so that: $\frac{r^2}{2\nu t} = 1$

$$r = a = \sqrt{2\nu t} \quad (11)$$

According to (11), the vortex grows in size while according to (10), it decays in strength with time.

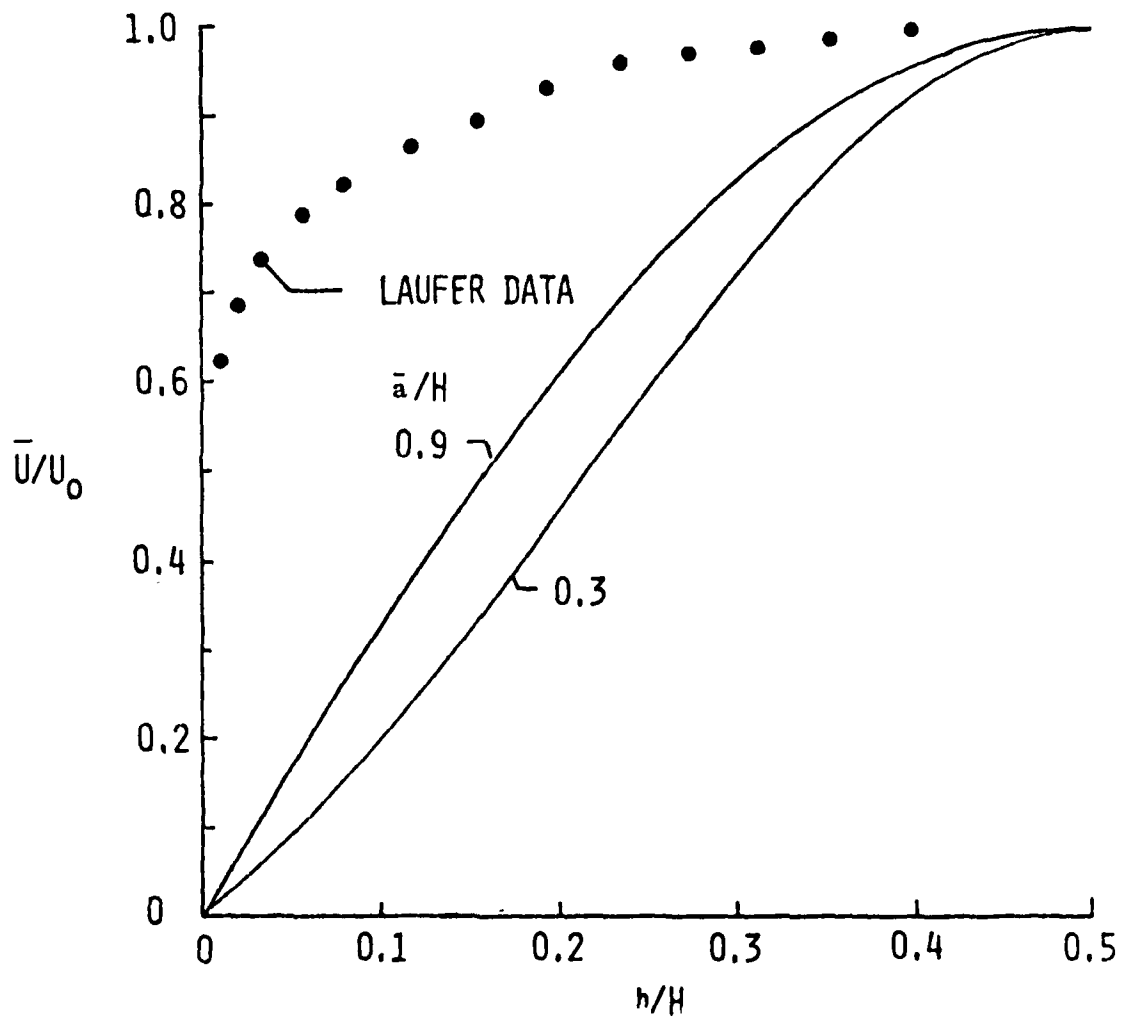
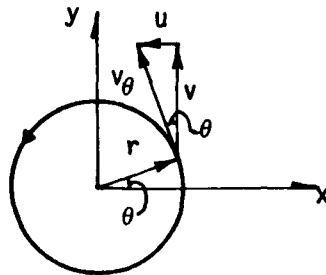


Figure 8. Mean Velocity Profiles Computed Using Uniform Vortex Properties.

The vortex tangential velocity can be expressed as axial and lateral components by using the following transformations:

Vortex Coordinates



$$u = -v_{\theta} \sin \theta = -v_{\theta} n \frac{y}{r}$$

$$v = v_{\theta} \cos \theta = v_{\theta} n \frac{x}{r}$$

$$u = -Bn \frac{y}{t^2} e^{-\frac{x^2+y^2}{4vt}} \quad (12a)$$

$$v = Bn \frac{x}{t^2} e^{-\frac{x^2+y^2}{4vt}} \quad (12b)$$

These velocity components are then transformed to the coordinate system "fixed" to the channel.

$$u = Bn \frac{y}{t^2} e^{-\frac{(+X_0+Ut)^2+Y^2}{4vt}} \quad (13a)$$

$$r = -Bn \frac{+X_0+Ut}{t^2} e^{-\frac{(+X_0+Ut)^2+Y^2}{4vt}} \quad (13b)$$

where: $x = -X_0 + Ut$

$X_0 =$ station where vortex originates

The vortex size therefore can be defined in terms of the distance across the channel.

The integral equation in Table II begins with the fluctuation of a single vortex. The time interval represents the time averaged influence for a single vortex. The vortex spin direction is chosen as clockwise in the lower half part of the duct and counter-clockwise in the upper half, see Figure 6. The basis for this assumption is the observation that a velocity decays below the average velocity near the wall, but is above average at the channel centerline. The vortex strength ($V_{\theta m}$) and size (a) are defined as functions from the lower wall.

The last unknown variable is the vortex flux (N). The flux rate can be specified by using a stability criteria, as shown in Table III. The final expression (III-1) relates the flux to the local velocity (U) and vortex size (a) variation across the channel.

The development for the mean velocity profile is presented in Table IV. This is the solution of equation (II-4) using equation (I-1) for the perturbation in the axial direction. The flux rate expression (III-1) is also used. The final result:

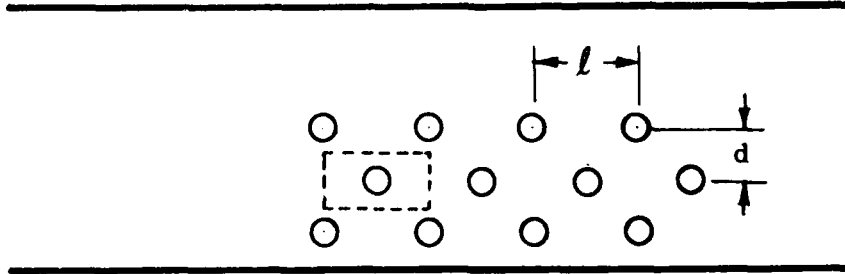
$$\frac{\bar{U}}{U_0} = \int_{-h/H}^{\frac{H-h}{H}} \frac{3.56 \sqrt{2e\pi}}{c_s^2} n \left(\frac{V_{\theta m}}{U_0} \right) \left(\frac{Y}{a} \right) e^{-\frac{1}{2} \left(\frac{Y}{a} \right)^2} d \left(\frac{Y}{a} \right) \quad (17)$$

must still be integrated with respect to distance across the channel. The integration limits are shown in Table I where Y/H is the variable of integration. The variation of vortex size (a/H) and strength ($V_{\theta m}/U_0$) are to be specified as functions of h/H , the distance from the lower wall. Typical results obtained are discussed in the next section.

The integral equations for three unsteady velocity correlation terms are presented in Table V. These derivations include the root-mean-square levels of the axial ($\sqrt{u'^2}/U_0$) and lateral ($\sqrt{v'^2}/U_0$) velocity perturbations and the cross correlation term $\overline{u'v'}/U_0^2$. The cross correlation term is an odd function of $\left(\frac{Y}{a}\right)$ and therefore yields zero. This assumes that time averaging the sum of vortex influence is the same as summing the vortex influence and then taking the time average. A finite answer can be obtained by considering the absolute value of the function with time. Typical results will be presented in the Data/Analysis section.

Integral equations were also developed for the unsteady terms in the Turbulent Kinetic Energy equation (Table VI). This topic is discussed later herein.

TABLE III
 Number of Vortices in 2-D Duct



Assume, that on the average, vortices will align themselves as shown schematically above, with spacings of l and d . Then,

$$\text{Number of vortices/unit area} = \frac{1}{l \cdot d}$$

$$\text{Number of vortices/unit Time} = \Delta N = \frac{1}{l \cdot d} \cdot U \Delta y$$

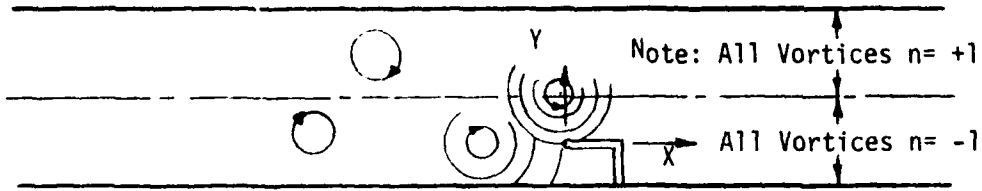
The spacing ratio, l/d , can be obtained by imposing a stability criteria on the vortex rows as, for example, in Milne-Thompson's Theoretical Hydrodynamics, p. 378, where,

$$\frac{l}{d} = 3.56$$

Further assume that $l \propto a$, $l = C_s a$. Then $\Delta N = \frac{3.56 U \Delta y}{l^2}$ and in the limit:

$$dN = \frac{3.56 U dy}{C_s^2 a^2} \tag{III-1}$$

TABLE IV
Time Average Velocity Induced By Vortices



Velocity induced by vortex "i" at probe:

$$u_i(t) = n v_{Om_i} \left(\frac{Y_i}{a_i}\right) e^{-1/2 \left\{ \left(\frac{U_i t}{a_i}\right)^2 + \left(\frac{Y_i}{a_i}\right)^2 - 1 \right\}} \quad (I-1)$$

The time average velocity induced will be:

$$\bar{u}_i = \frac{1}{T} \int_{-T/2}^{T/2} u_i(t) dt = \frac{n}{T} v_{Om_i} \left(\frac{Y_i}{a_i}\right) \sqrt{2\pi} \frac{a}{u} e^{-1/2 \left\{ \left(\frac{Y_i}{a_i}\right)^2 - 1 \right\}} \quad (IV-1)$$

The time averaged velocity induced by all vortices will be N times that induced by a single vortex, thus:

$$\bar{u} = \int d\bar{u} = \int \bar{u}_i T dN$$

$$\text{where } dN = \frac{3.56 \bar{u}}{C_s^2 a^2} dY \quad (III-1)$$

$$d\bar{u} = \frac{3.56 \bar{u}}{C_s^2 a^2} n v_{Om} \frac{Y}{a} \sqrt{2\pi} \frac{a}{u} e^{-1/2 \left\{ \left(\frac{Y}{a}\right)^2 - 1 \right\}} dY \quad (IV-2)$$

Simplifying, the average velocity becomes:

$$d\bar{u} = \frac{3.56 \sqrt{2\pi} e}{C_s^2} n v_{Om} \frac{Y}{a} e^{-1/2 \left(\frac{Y}{a}\right)^2} \frac{dY}{a} \quad (IV-3)$$

TABLE V

VELOCITY CORRELATION TERMS

$$\overline{u^2} = N \int u(t) u(t) dt$$

$$\int u^2(t) dt = \int v_{0m}^2 \left(\frac{y}{a}\right)^2 e^{-\left[\left(\frac{ut}{a}\right)^2 + \left(\frac{y}{a}\right)^2 - 1\right]} dt \quad (V-1)$$

$$= v_{0m}^2 \left(\frac{y}{a}\right)^2 \sqrt{\pi} \left(\frac{a}{u}\right) e^{-\left[\left(\frac{y}{a}\right)^2 - 1\right]} \quad (V-2)$$

$$d\overline{u^2} = \left[\int u^2(t) dt \right] dN$$

$$d\overline{u^2} = \frac{3.56u}{c_s^2 a^2} v_{0m}^2 \left(\frac{y}{a}\right)^2 \sqrt{\pi} \left(\frac{a}{u}\right) e^{-\left[\left(\frac{y}{a}\right)^2 - 1\right]} dy \quad (V-3)$$

$$d\overline{u^2} = \frac{3.56e\sqrt{\pi}}{c_s^2} v_{0m}^2 \left(\frac{y}{a}\right)^2 e^{-\left(\frac{y}{a}\right)^2} \frac{dy}{a} \quad (V-4)$$

$$\overline{v^2} = N \int v(t) v(t) dt$$

$$\int v^2(t) dt = \int v_{0m}^2 \left(\frac{ut}{a}\right)^2 e^{-\left[\left(\frac{ut}{a}\right)^2 + \left(\frac{y}{a}\right)^2 - 1\right]} dt \quad (V-5)$$

$$= v_{0m}^2 \left(\frac{u}{a}\right)^2 \frac{e}{2} \left(\frac{a^2}{u}\right) \frac{a}{u} \sqrt{\pi} e^{-\left(\frac{y}{a}\right)^2}$$

$$d\overline{v^2} = \left[\int v^2(t) dt \right] dN$$

$$d\overline{v^2} = \frac{3.56u}{c_s^2 a^2} v_{0m}^2 \frac{e\sqrt{\pi}}{2} \left(\frac{a}{u}\right) e^{-\left(\frac{y}{a}\right)^2} dy$$

$$d\overline{v^2} = \frac{1.78e\sqrt{\pi}}{c_s^2} v_{0m}^2 e^{-\left(\frac{y}{a}\right)^2} \frac{dy}{a} \quad (V-6)$$

TABLE V

VELOCITY CORRELATION TERMS (CONTINUED)

USING ACTUAL VALUE:

$$\overline{u'v'} = N \int_{-\infty}^{\infty} u(t)v(t) dt \quad (V-7)$$

$$\begin{aligned} \int u(t)v(t) dt &= \int_{-\infty}^{\infty} -v_{0m}^2 \left(\frac{y}{a}\right) \left(\frac{ut}{a}\right) e^{-\left[\left(\frac{ut}{a}\right)^2 + \left(\frac{y}{a}\right)^2 - 1\right]} dt \\ &= \int_{-\infty}^{\infty} t e^{-t^2} dt = 0 \end{aligned} \quad (V-8)$$

$$\overline{u'v'} = 0$$

Note: This assumes that time averaging the sum of vortex influence is same as summing the vortex influence and taking time average. This is not true and thus answer is too low.

USING ABSOLUTE VALUE:

$$\overline{|u'| |v'|} = N \int |u(t)| |v(t)| dt \quad (V-9)$$

$$\begin{aligned} \int |u(t)| |v(t)| dt &= 2 \int_0^{\infty} v_{0m}^2 \left(\frac{y}{a}\right) \left(\frac{ut}{a}\right) e^{-\left[\left(\frac{ut}{a}\right)^2 + \left(\frac{y}{a}\right)^2 - 1\right]} dt \\ &= 2 e v_{0m}^2 \left(\frac{y}{a}\right) \frac{u}{a} \left(\frac{-a^2}{2u^2}\right) e^{-\left(\frac{y}{a}\right)^2} \end{aligned}$$

$$d|u'| |v'| = -\frac{3.56u}{c_s^2 a^2} 2 e v_{0m}^2 \left(\frac{y}{a}\right) \left(\frac{a}{2u}\right) e^{-\left(\frac{y}{a}\right)^2} dy$$

$$d|u'| |v'| = -\frac{3.56e}{c_s^2} v_{0m}^2 \left(\frac{y}{a}\right) e^{-\left(\frac{y}{a}\right)^2} \frac{dy}{a} \quad (V-10)$$

Note: This assumes influence of one vortex on another is very (all!) important. Thus answer is probably too high.

TABLE VI
TURBULENT KINETIC ENERGY EQUATION TERMS

$$\frac{\partial}{\partial y} (\overline{p v'} + \frac{1}{2} \overline{g^2 v'}) \quad \text{diffusive}$$

$$\begin{aligned} \overline{p v'} + \frac{1}{2} \overline{g^2 v'} &= \overline{p v'} + \frac{1}{2} (\overline{u'^2 v'} + \overline{v'^3}) \\ &= N \int p(t) v(t) dt + \frac{N}{2} \int [u(t)]^2 v(t) dt \\ &\quad + \frac{N}{2} \int [v(t)]^3 dt \end{aligned}$$

$$\begin{aligned} d(\overline{p v'} + \frac{1}{2} \overline{g^2 v'}) &= \frac{1.187 e^{3/2} n}{c_s^2} \rho V_{om}^3 e^{-3/2 (y/a)^2} d(y/a) \\ &\quad + \frac{1}{2} \rho \left(\frac{2}{3}\right) \frac{3.56 e^{3/2} n^3 V_{om}^3}{c_s^2} \left(\frac{y}{a}\right)^2 e^{-3/2 (y/a)^2} d(y/a) \\ &\quad + \frac{1}{2} \rho \left(\frac{4}{9}\right) \frac{3.56 e^{3/2} n^3 V_{om}^3}{c_s^2} e^{-3/2 (y/a)^2} d(y/a) \end{aligned}$$

$$\mu \left[\left(\frac{\partial u'}{\partial y}\right)^2 + 2 \left(\frac{\partial v'}{\partial y}\right)^2 \right] \quad \text{dissipation}$$

$$\begin{aligned} \mu \left[\left(\frac{\partial u'}{\partial y}\right)^2 + 2 \left(\frac{\partial v'}{\partial y}\right)^2 \right] &= \mu \int \frac{3.56 e \sqrt{\pi}}{c_s^2} \left(\frac{V_{om}}{a}\right)^2 \left[1 - \left(\frac{y}{a}\right)^2\right] e^{-\left(\frac{y}{a}\right)^2} d\left(\frac{y}{a}\right) \\ &\quad + \mu \int \frac{3.56 e \sqrt{\pi}}{c_s^2} \left(\frac{V_{om}}{a}\right)^2 \left(\frac{y}{a}\right)^2 e^{-\left(\frac{y}{a}\right)^2} d\left(\frac{y}{a}\right) \end{aligned}$$

2.3 DISTRIBUTION OF VORTEX PROPERTIES FOR TWO-DIMENSIONAL FLOW

The turbulent flow model is composed of a series of random vortices convected by the local flow. The flow about each individual vortex is essentially a steady state flow field as described in a coordinate system fixed to the vortex. The flow field for each vortex extends across the entire channel. The single vortex circular motion appears as a fluctuation or turbulence as it passes a point fixed to the channel. The flow at this observation point is influenced by the flow field from every vortex that passes down the channel. In other words, the turbulence at a point in the channel depends on the characteristics of vortices all across the channel. Therefore, it is necessary to define the distribution of vortex properties across the two-dimensional channel.

2.3.1 Vortex Distributions from Measured Unsteady Pressures

As described in Section 2.1, the Turbulent Flow Model can be used to compute the distribution of vortex properties. Measurement of the unsteady pressure fluctuations can yield a root-mean-square (RMS) level and power spectral density (PSD) function at various points across the channel. The RMS is a measure of the average vortex strength and the PSD shape determines the mean vortex size. This procedure requires measurement of the turbulence in terms of the unsteady total pressure fluctuations.

This type of data was not available for the current study. Therefore, the primary focus was at finding the typical distributions of the vortex properties that yielded unsteady velocity correlation terms that matched the test data of Laufer, Reference 2.

2.3.2 Distribution of Vortex Properties for Analytical Solution

The mean velocity profile, Equation (17), and also the turbulence terms distributions depend on the distribution of vortex properties across the channel. For a fully exact treatment, each vortex property should be defined by a probability density function. This permits each property to have any value within its acceptable range with assigned probabilities for each value. However, for this analysis, each vortex property is assumed to have only one value, its average value, at each location across the channel. Each vortex parameter is discussed briefly.

The vortex axial location is assumed to be uniform. This parameter is represented by the Ut/a term in equation (1-1) and is included as the dt variable of integration in Equation (17). Each eddy is convected by the local velocity, so that $X = Ut$.

The vortex spin direction is also treated as being constant with the following conditions. In the lower half of the channel all eddies are assumed to spin in the clockwise direction ($n = -1$) and in the upper half of the channel all vortices spin counter-clockwise ($n = +1$); see Table 1.

The vortex flux rate expression was derived using the Milne-Thompson stability criteria which is based on rows of vortices of alternating spin direction. This is applicable because the vortices in the turbulent flow are random. The restriction in spin direction imposed in the preceding paragraph is similar to using the average value of vortex size and strength.

The vortex maximum tangential velocity ($V_{\theta m}/U_0$) is described as a function of location across the channel (h/H). Four velocity distributions used early in the study are shown in Figure 9. The vortex strength is expressed as the ratio of maximum tangential velocity ($V_{\theta m}$) to the channel maximum velocity (U_0). Referring to Table I, the distance from the lower wall is h and the channel width (height) is H . The velocity distributions are shown from the wall to the channel centerline only and are assumed to be symmetrical about the channel centerline. Distribution V1 is similar to the classical turbulent boundary layer shear stress distribution. The velocity is zero at the duct centerline and increases linearly toward the wall, then decays rapidly to zero at the surface. Distribution V2 is more or less arbitrary, it has a finite value at the centerline but is zero at the wall. Distribution V3 is directly proportional to the derivative of the Laufer data mean velocity profile and is not zero at the wall, and V4 is a uniform distribution. Additional vortex strength distributions were developed during the study and will be presented in the DATA/ANALYSIS COMPARISON section 2.5.

The vortex size (a/H) is also described as a function of location across the channel (h/H). Four vortex size distributions used early in the study are shown in Figure 10. The vortex size, (\bar{a}), is presented as a ratio of the channel width (H). And the distribution is specified only from the lower wall to the channel centerline and is also assumed to be symmetrical about the centerline. The A2 distribution, with $\bar{a}/H = 0.5$, is similar to that used previously for the closed solution. Distribution A1 is completely arbitrary but reflects the empirical notion that the vortices are small near the wall and increase in size toward the channel centerline. Distribution A3 was derived as a first order match of the Laufer mean velocity profile data. Distribution A4 is the average of A1 and A3. Again, other vortex size distributions were developed during the study and discussed in the DATA/ANALYSIS COMPARISONS section.

The last variable in Equation (17) is the lateral location Y . Note: See model in Table I, that the variable Y is measured from some "sensing" point located across the channel. The range of values varies from $-h$ to $H-h$. The parameter h specifies a point in the channel and corresponds to the location of the "sensing" point. The vortex size (a/H) and strength ($V_{\theta m}/U$) distributions are specified in terms of h/H . The variable Y then defines the contributions from vortices all across the channel at point h . The vortex size and strength distributions are specified only for one-half of the channel (the other half is assumed to be symmetrical). The lateral position integration variable (Y), however, extends from wall to wall. This is required because all vortices in the channel contribute to the turbulence at each point in the flow field. This range of the Y variable permits the vortex spin direction to change at the channel centerline.

The above solution procedure for the mean velocity profile is also applicable to the other turbulence terms. Typical results obtained are shown in the DATA/ANALYSIS COMPARISONS section.

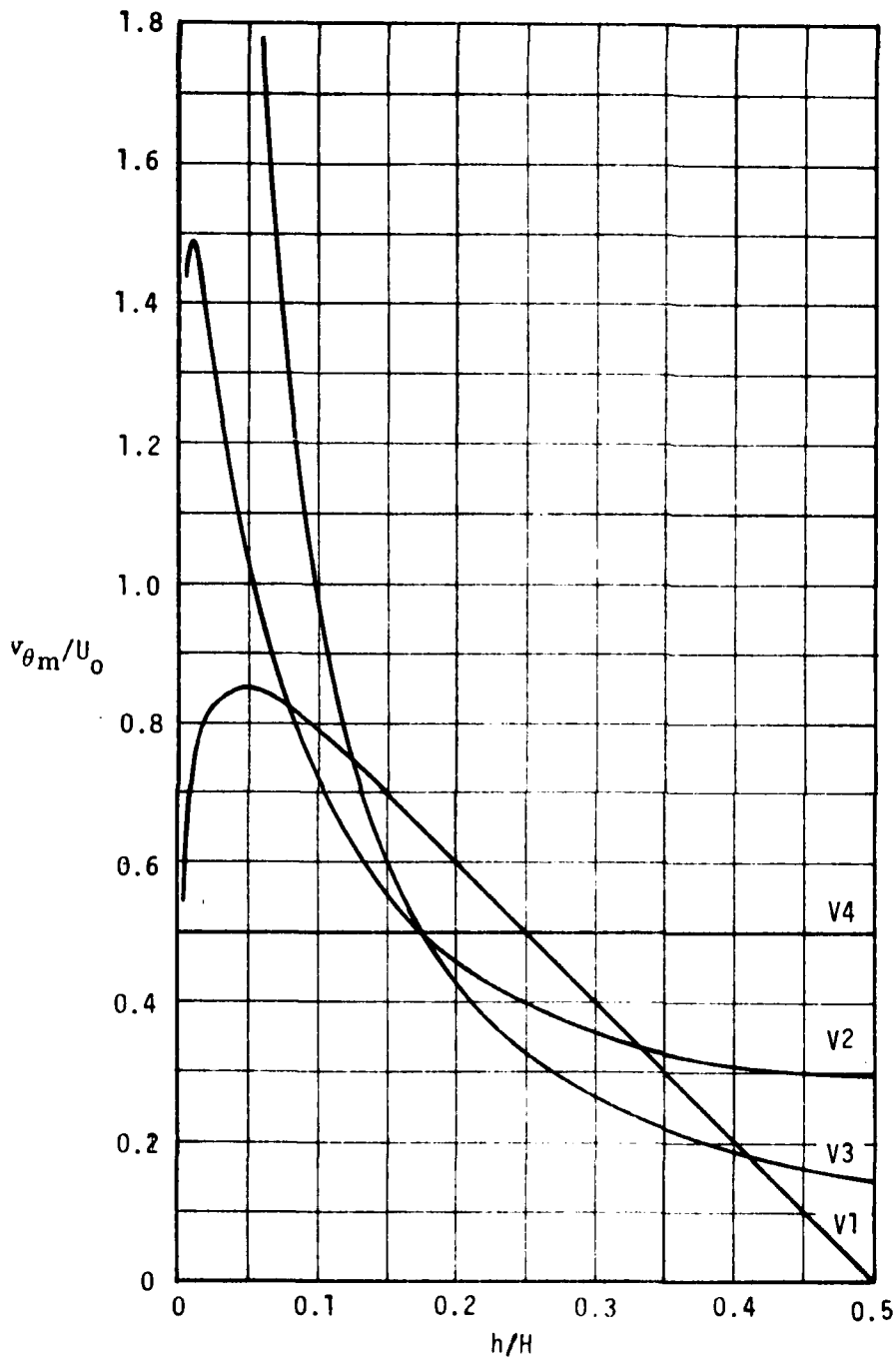


Figure 9. Vortex Strength Distributions.

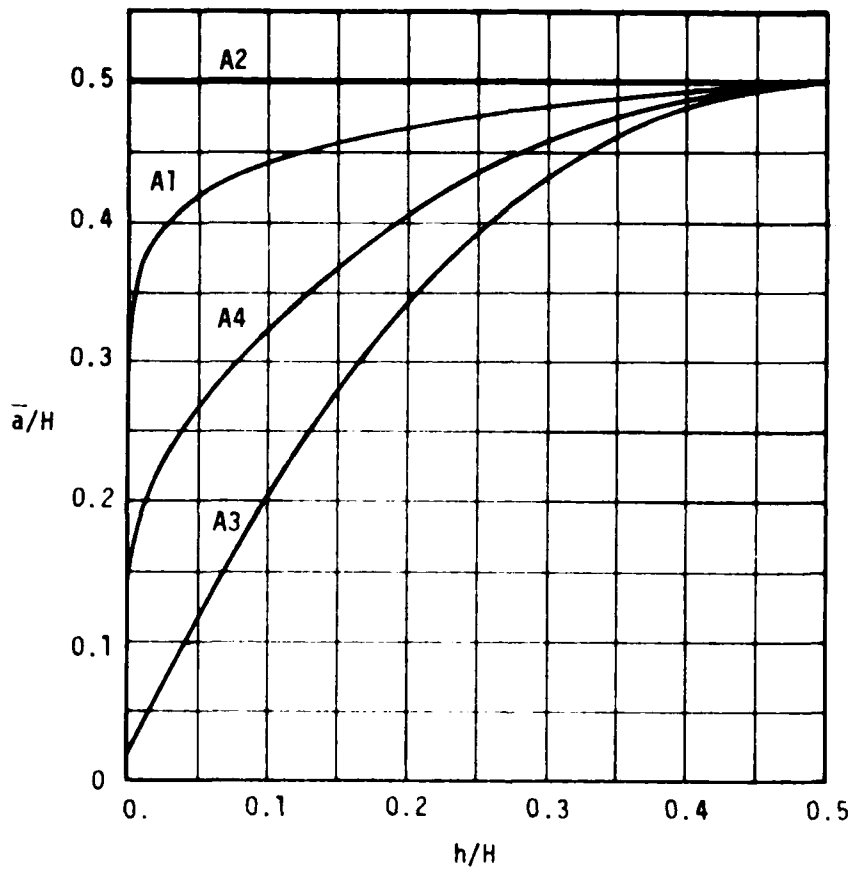


Figure 10. Vortex Size Distributions.

2.4 EFFECTS OF BOUNDARY CONDITIONS

The objective of the current study is to obtain a solution of the Reynolds Equation of Motion for turbulent flow using a statistical vortex turbulence closure. This link is provided by the Turbulent Flow Model, developed in Reference 1 and applied herein. The Reynolds Equation defines the steady state flow field in terms of both steady state and time averaged unsteady velocity components. Historically, the unsteady velocity components have been related by use of the "mixing lengths" or "eddy viscosity". The Reynolds stresses are defined in terms of these "constants". In the current study, the Reynolds stresses are defined directly in terms of the turbulent flow characteristics.

The solution procedure based on the vortex started impulsively, Section 2.2.1.2, required an additional equation in order to determine the vorticity strength (B). The Turbulent Kinetic Energy Equation was formulated for this initial use. Although this solution procedure was not completed, solutions for the TKE terms were conducted and are also discussed in this section.

2.4.1 Reynolds Equation of Motion

The Reynolds Equations of Motion for fully developed two-dimensional flow are derived from Section 2.2. For this flow, gradients in the axial direction of the mean flow and turbulence quantities vanish. Application of the continuity equation for the mean flow and the impervious wall boundary condition shows that the mean transverse velocity components are zero across the channel. This removes the continuity equation from the set of governing equations. The resultant simplified governing equations may be written in dimensionless form as:

$$\frac{1}{Re_0} \frac{\partial^2 \bar{u}}{\partial y^2} - \frac{\partial}{\partial y} (\overline{u'v'}) = \frac{1}{2} \frac{\partial \bar{p}}{\partial x} \quad (18)$$

$$\frac{\partial}{\partial y} (\overline{v'^2}) = -1/2 \frac{\partial \bar{p}}{\partial y} \quad (19)$$

where the dimensionless variables are defined as follows:

$$\begin{aligned} x &= \frac{x^*}{H} & \bar{u} &= \frac{\bar{u}^*}{u_0} & u' &= \frac{(u')^*}{u_0} & \bar{p} &= \frac{p^* - p_0}{1/2 \rho u_0^2} \\ y &= \frac{y^*}{H} & \overline{u'v'} &= \frac{\overline{u'v'^*}}{u_0^2} & v' &= \frac{(v')^*}{u_0} & Re_0 &= \frac{\rho u_0 H}{\nu} \end{aligned} \quad (20)$$

where, u_0 and p_0 are reference quantities and an asterisk denotes a dimensional quantity. Equation (19) may be integrated to yield the following algebraic equation for the pressure distribution across the channel:

$$\bar{p} = \bar{p}_w - 2(\overline{v'^2}) \quad (21)$$

where \bar{p}_w is the local (dimensionless) wall static pressure. Differentiating equation (21) yields)

$$\frac{\partial \bar{p}}{\partial x} = \frac{d\bar{p}_w}{dx} \quad (\text{since } \bar{p}_w = f(x) \text{ only})$$

Substituting this result in equation (18) and integrating yields the following result upon application of the symmetry conditions for the mean flow and fluctuating components

(i.e., $\frac{\partial \bar{u}}{\partial y} = \overline{u'v'} = 0$ at the centerline):

$$\frac{d\bar{u}}{dy} = Re_0 \left\{ \overline{u'v'} + y/2 \frac{d\bar{p}_w}{dx} \right\} \quad (22)$$

Equation (22) may be integrated (numerically) with the boundary conditions $\bar{u} = \overline{u'v'} = 0$ at the wall if an expression for $\overline{u'v'}$ as $f(y)$ is known. Such a functional expression can be obtained from the Turbulent Flow Model Solution. Typical results with this numerical procedure are given below.

At present the wall pressure gradient must be known in order to integrate the equation. This is desirable since the $\overline{u'v'}$ distribution will be unconstrained during the turbulence model development. When a satisfactory model is obtained, the pressure gradient term can be iterated to meet the equivalent conditions:

$$\dot{m} = \int_H \rho \bar{u} \, dy \quad \text{or} \quad \frac{\bar{u}}{u_{\max}} = 1 \quad \text{at the centerline.}$$

A computer program was written to solve equation (22). Since the equation is simply an ordinary differential equation for the mean velocity U , any suitable numerical algorithm may be used. The present computer program uses the multistep method by Shampine and Gordon, reference 6. The program was checked for a laminar and turbulent flow case.

The laminar flow is obtained by setting $\overline{u'v'} = 0$. An exact analytical solution exists for this flow and is given by:

$$\frac{\bar{u}}{U_0} = 1 - \left(\frac{y}{H/2}\right)^2 \quad \frac{dp}{dx} = \frac{-16}{Re_0}$$

A comparison of the analytical and numerical solutions in Figure 11 for $Re_0 = 30800$ shows that the solutions are identical. Although a laminar flow probably could not be maintained physically at this high Reynolds number, this does not affect the solution of the equation.

The turbulent flow case considered uses the data of Laufer for a Reynolds number of 24600 (or a half width Reynolds number of 12300). The $\overline{u'v'}$ distribution was interpolated by cubic splines from the measured data that was obtained by hot wire anemometry. The resultant calculated mean velocity profile is compared to the measured profile in Figure 12 and shows excellent agreement. Initial attempts to calculate the mean velocity profile shown in Figure 12 revealed extreme sensitivity to the $\overline{u'v'}$ profile, especially in the near wall region where gradients are very large.

The Reynolds stress term is defined by equation (11-3), Table 11, in terms of the Turbulent Flow Model. The integral solution procedure used for this mean velocity profile, equation (17), is also applicable to the Reynolds stress term. Results obtained are presented in Section 2.5 and can be used in the preceding technique to obtain solution of the Reynolds Equations of Motion.

2.4.2 Turbulent Kinetic Energy (TKE) Equation

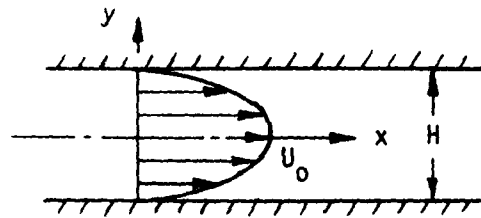
The method of specifying the turbulent flow model by the vortex started impulsively, Section 2.2.1.2, required additional constraints for proper closure. It was found that this closure could be achieved by using the turbulent kinetic energy equation. And although the solution method was abandoned due to the complexity in the integration procedure, the TKE was retained. The TKE offers additional means of verifying the Turbulent Flow Model solution for turbulent flow in a 2-D channel.

The TKE has the following form for the 2-D channel flow.⁷

$$-\overline{u'v'} \frac{\partial u}{\partial y} - \frac{\partial}{\partial y} (\overline{pv'} + \frac{1}{2} \overline{q^2 v'}) = \mu \left[\left(\frac{\partial u}{\partial y} \right)^2 + 2 \left(\frac{\partial v}{\partial y} \right)^2 \right] \quad (23)$$

The first item on the left hand side is the turbulence production term. Turbulence is created by the Reynolds stresses working on the mean velocity profile. The second term on the left hand side accounts for diffusion of the turbulence due to the pressure and velocity gradient. These two parts are combined here similarly to Laufer's approach. This term accounts for the transfer of turbulence into (and/or from) a region in the flow. The right hand term accounts for the dissipation of turbulence. The vortices that constitute the turbulence yield their energy as they disappear.

The three terms in the TKE, equation (23), represent energy levels. Laufer presents these terms as the change in energy per unit time transferring into and out from a unit volume at each point across the channel. A similar approach has been followed herein. The Turbulent Flow Model was used to generate the correlations in the diffusive and dissipation terms. Results obtained are presented in the DATA/ANALYSIS COMPARISONS section. Since this energy relation must also be satisfied, it can also be used as a further check on the validity of the Turbulent Flow Model.



$$Re = 30800$$

$$dp/dx = -.000519$$

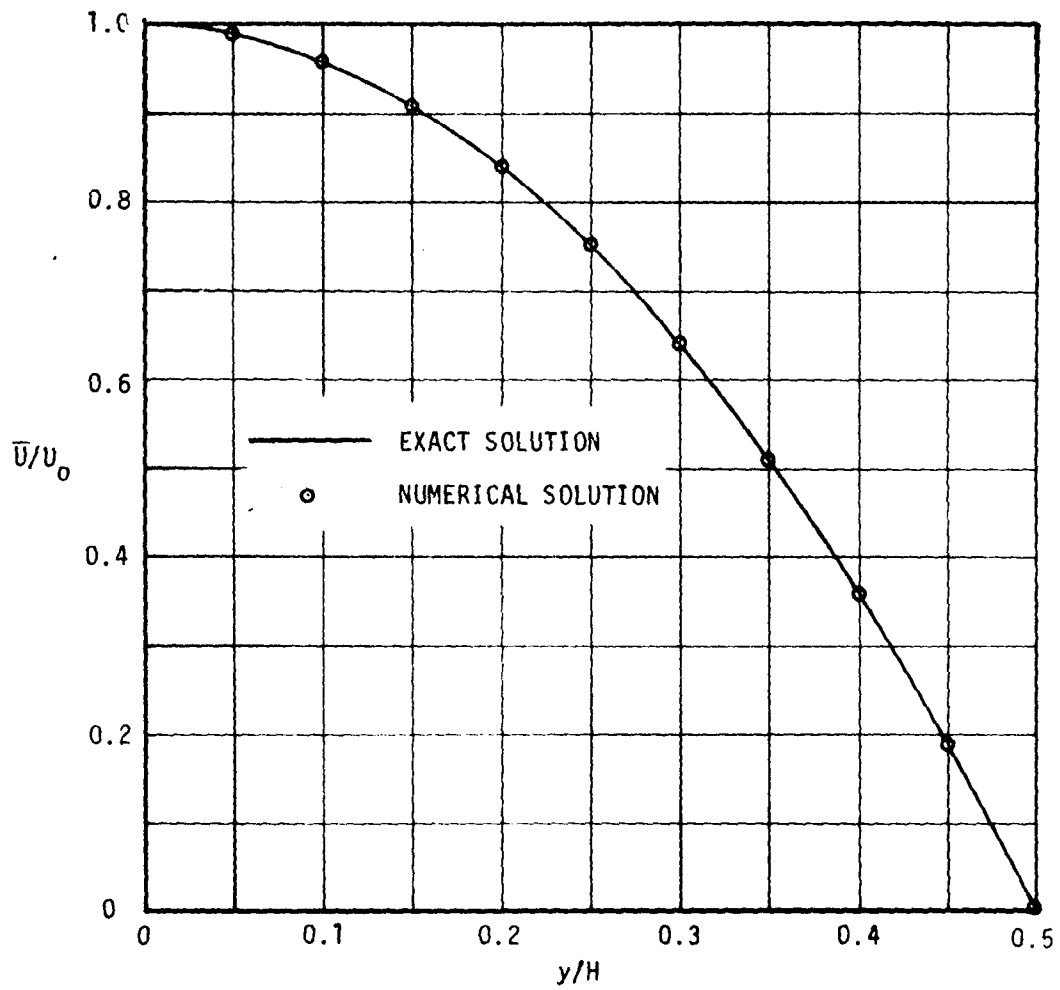
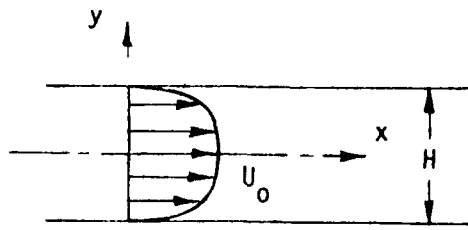


Figure 11. Fully Developed 2-D Channel Incompressible Laminar Flow



$$Re = 24600$$

$$dp/dx = -.0072$$

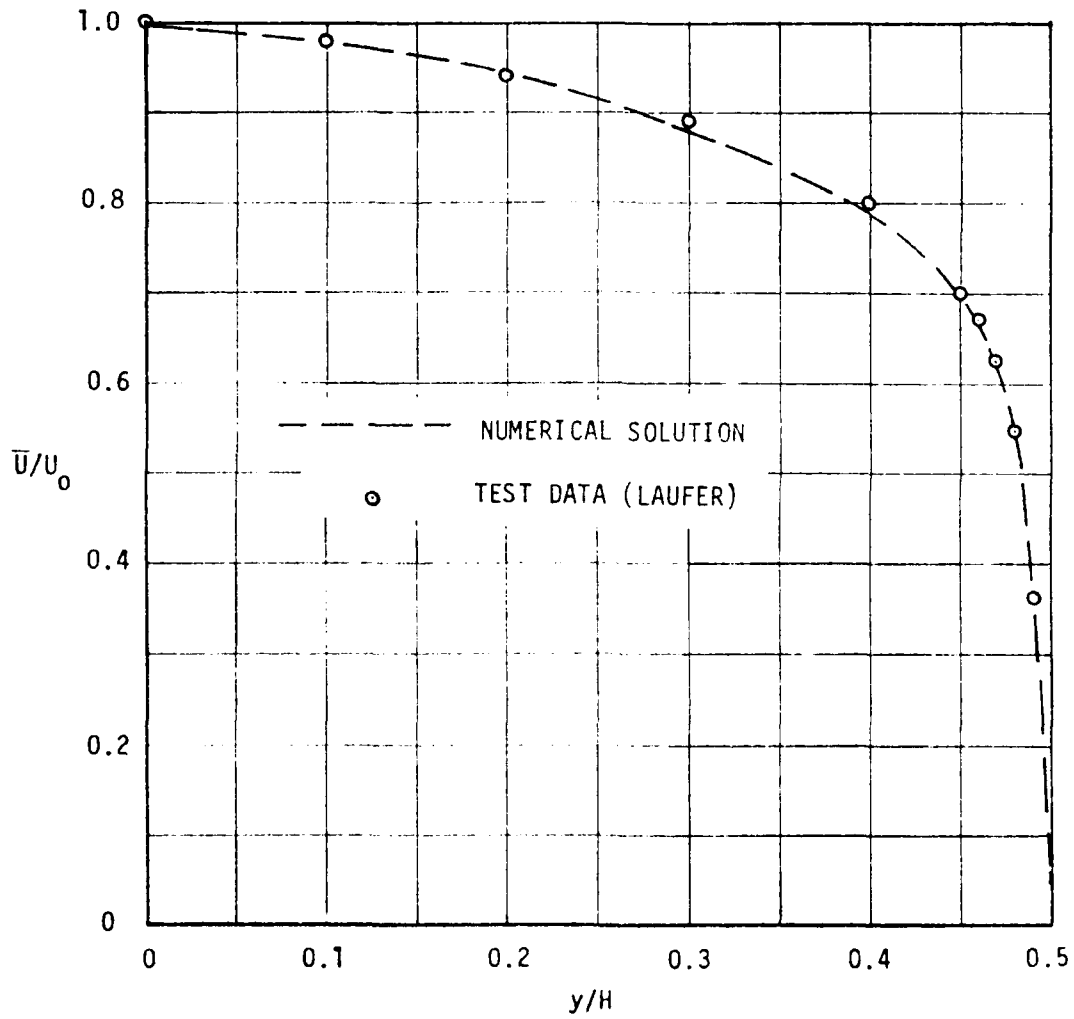


Figure 12. Fully Developed 2-D Channel Incompressible Turbulent Flow

2.5 DATA/ANALYSIS COMPARISONS

Results obtained with the Turbulent Flow Model are compared with the measured results published by Laufer.⁴ First a brief review of the test and the type of measurements made is presented. Then comparisons are made for mean velocity profiles, Reynolds stresses, and TKE terms.

2.5.1 Laufer's Measurements

Laufer² used both a 1-inch and 5-inch channel for measuring the unsteady velocity fluctuations. For the 5-inch tunnel configuration the recorded measurements at three Reynolds numbers: 12,300, 30,800, and 61,600. These Reynolds numbers are based on the maximum duct velocity (U_0) and the duct half-width (2.5 inch). A summary of the Laufer data is presented in Figure 13. In these figures the velocities are normalized by the maximum duct velocity (U_0) and are plotted versus distance from the lower wall (h/H). The upper left chart shows the measured (symbols) mean velocity profiles. The exact laminar profile is included for reference. The upper right hand chart shows the cross-correlation term - both the measured values (symbols) and the values computed (lines) to satisfy the mean profiles. The lower charts show the unsteady velocity correlation measured root-mean-square values for the axial and lateral directions.

Laufer also computed the energy levels for the production, diffusive, and dissipation terms of the Turbulent Kinetic Energy (TKE) Equation. These energy levels are presented in Figure 14 for the Reynolds number = 30,800 case. The production term is zero at the channel centerline and increases as the wall is approached. The diffusive term is negative at the centerline and also increases as the wall is approached. The negative sign at the centerline indicates a gain in energy in this region. The dissipation term remains positive throughout and decreases toward the centerline. At any point in the channel, the total energy must be conserved. Therefore, the sum of production less diffusive less dissipation is zero, or:

$$\text{Production} - \text{Diffusive} - \text{Dissipation} = 0$$

2.5.2 Analytical Predictions

Some typical results obtained in the study are presented next. These comparisons include the various parameters for which test data were contained in Laufer's report. Among these parameters are: the mean velocity profile, the Reynolds stress term ($\overline{u'v'}$), the unsteady velocity correlation terms ($\overline{u'^2}$ and $\overline{v'^2}$) and the Turbulent Kinetic Energy equation energy balance terms.

2.5.2.1 Mean Velocity Profiles

The velocity perturbation due to a single vortex is given by equation (1-1). The turbulence properties depend directly on the number of vortices influencing the sensing probe. The vortex flux in a 2-D channel is derived in Table III, and the time average velocity induced by all the vortices is derived in Table IV. This approach is based on finding the velocity induced by a single vortex at a point (probe) and then finding the average velocity induced due to all the vortices contained in the flux developed in Table III. The resultant average velocity is then given by:

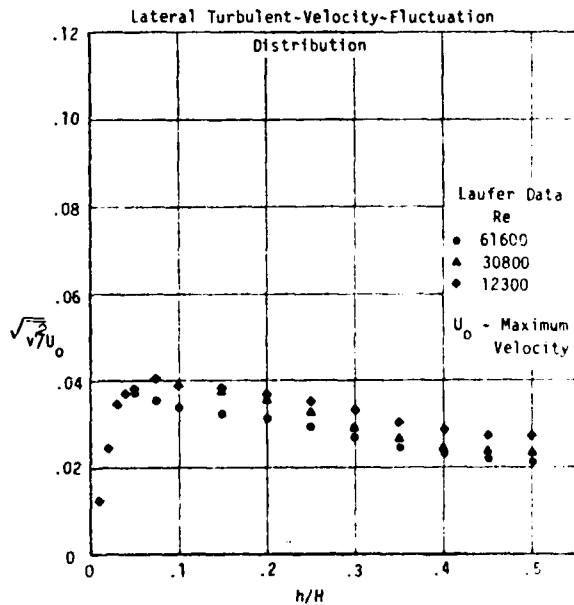
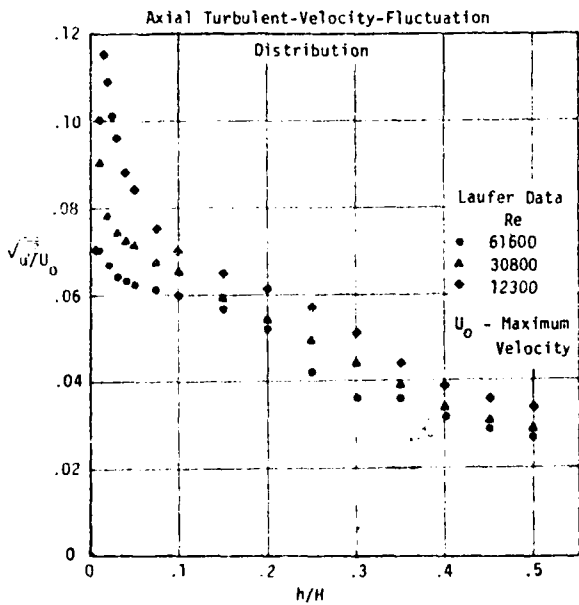
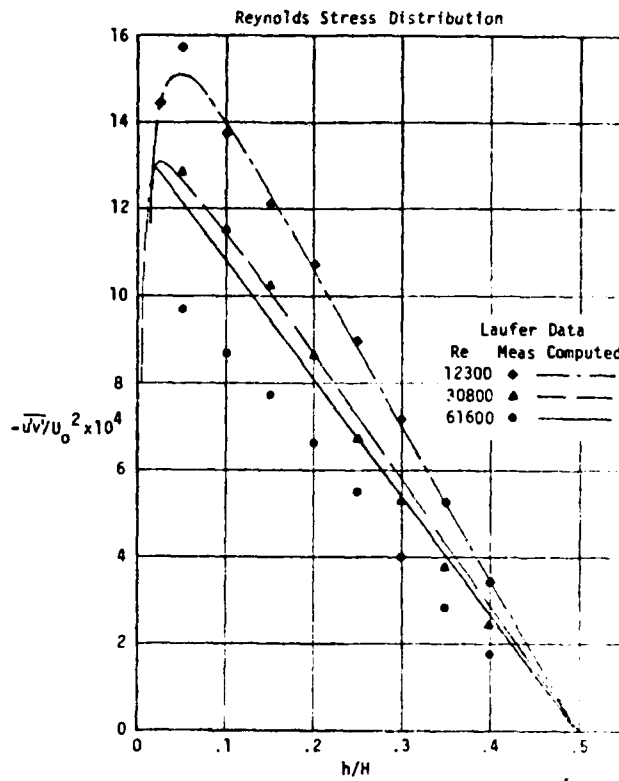
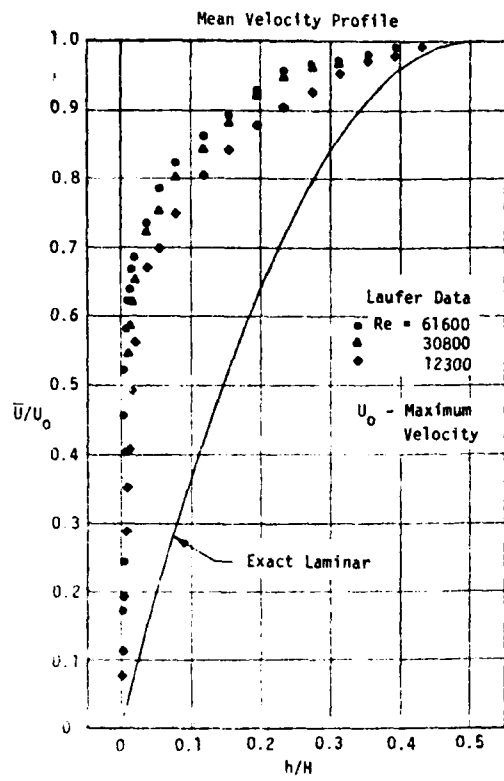


Figure 13. Summary of Turbulent Flow Data in 2-D Channel, Reference (2).

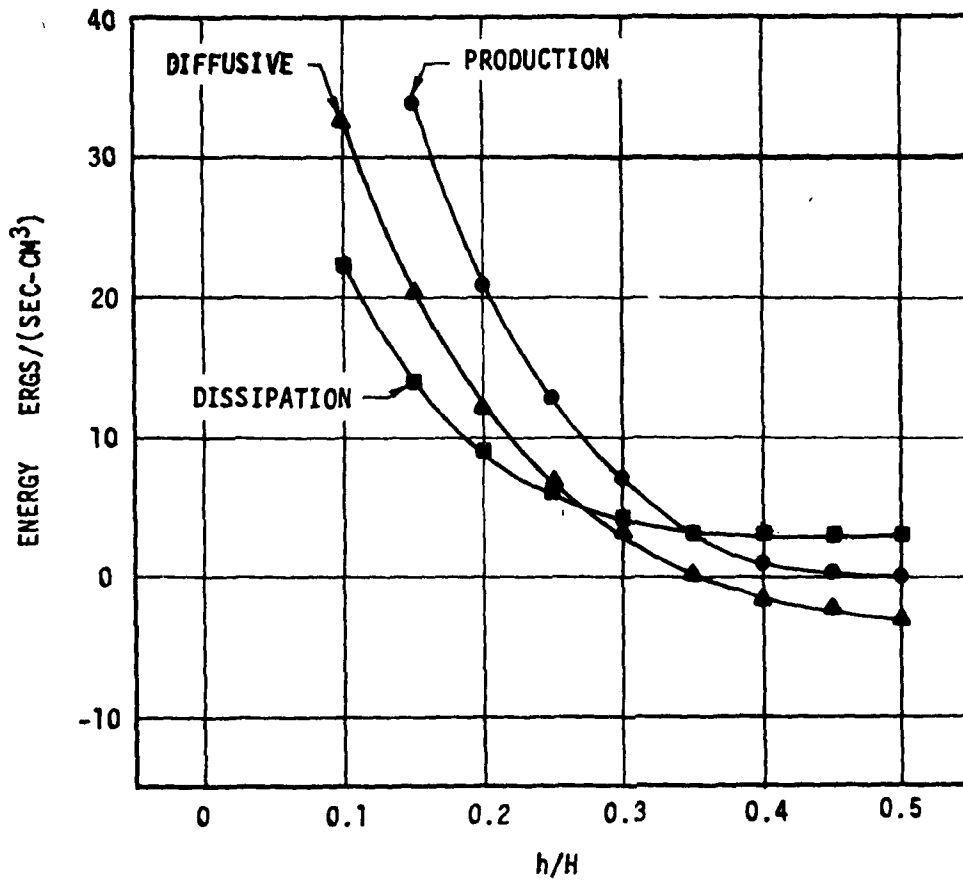


Figure 14. Turbulent Energy Balance Data, Reference (2).

$$\frac{\bar{U}}{U_0} = \int_{-h/H}^{\frac{H-h}{H}} \frac{3.56 \sqrt{2e\pi}}{c_s^2} n \left(\frac{V_{\theta m}}{U_0} \right) \left(\frac{Y}{a} \right) e^{-\frac{1}{2} \left(\frac{Y}{a} \right)^2} d \left(\frac{Y}{a} \right) \quad (17)$$

Equation (17) was solved by a numerical integration procedure. The variations of vortex strength ($V_{\theta m}/U_0$) and size (a/H) were specified as per Figures 9 and 10. Typical results are shown in Figure 15. Most of these resultant mean velocity profiles resemble the laminar profile. The A3V1 solution (i.e., by using vortex size distribution A3, Figure 10, and vortex strength distribution V1, Figure 9, indicates that there are distributions of vortex properties which will yield correct results.

2.5.2.2 Unsteady Velocity Correlation Terms

The Reynolds stress term and the unsteady velocity correlation terms are computed from expressions similar to Equation (17), as presented in Table V.

2.5.2.3 Turbulent Kinetic Energy Terms

The turbulent kinetic energy equation for fully developed two-dimensional channel flow is given as Equation (23). The first term, the production term, is based on the Reynolds stresses. The second term is the derivative of the pressure and velocity transport. The integral expressions for these terms are listed in Table VI. The right hand term of Equation (23) is the dissipation term and is also specified in Table VI.

2.5.3 Comparisons

The combination A2V4 represent the solution for constant vortex size and constant distributions. Results obtained with these distributions of vortex properties are shown in Figure 16. The mean velocity profile predicted is similar to a laminar profile. Note that although the Reynolds stress term distribution is similar in shape to the test data, the values are more than an order of magnitude high. The unsteady velocity correlation terms are also an order of magnitude high. The energy production and diffusive terms are three orders of magnitude too large. This is due to the laminar type profile.

The combination A3V1 solution yields mean velocity profile which is closer to the turbulent profile. The Reynolds stress and unsteady velocity correlation terms are reduced to less than a factor of ten high. The TKE production and diffusive terms are reduced to about an order of magnitude difference, too. These comparisons are shown in Figure 17.

A large number of vortex strength and size distributions were investigated during the study. Six strength and three size distributions used are shown in Figure 18. The velocity distributions shown all have the general properties of distribution V1, Figure 9. The effects of each distribution are discussed below. The three vortex size distributions shown in Figure 18(b) have the general characteristics of distribution A3, Figure 10. The initial slope ($d\bar{u}/dh$) is the principal variable. The net effect is to make A150 distribution almost linear and the A300 distribution full and flat. The following trends were observed. The magnitude of the Reynolds stress and the unsteady velocity terms depend directly on the vortex strength. The level is more significant than the distribution; the distribution is most important near the wall. The vortex strength distribution seems to have minor effect on the mean velocity profile.

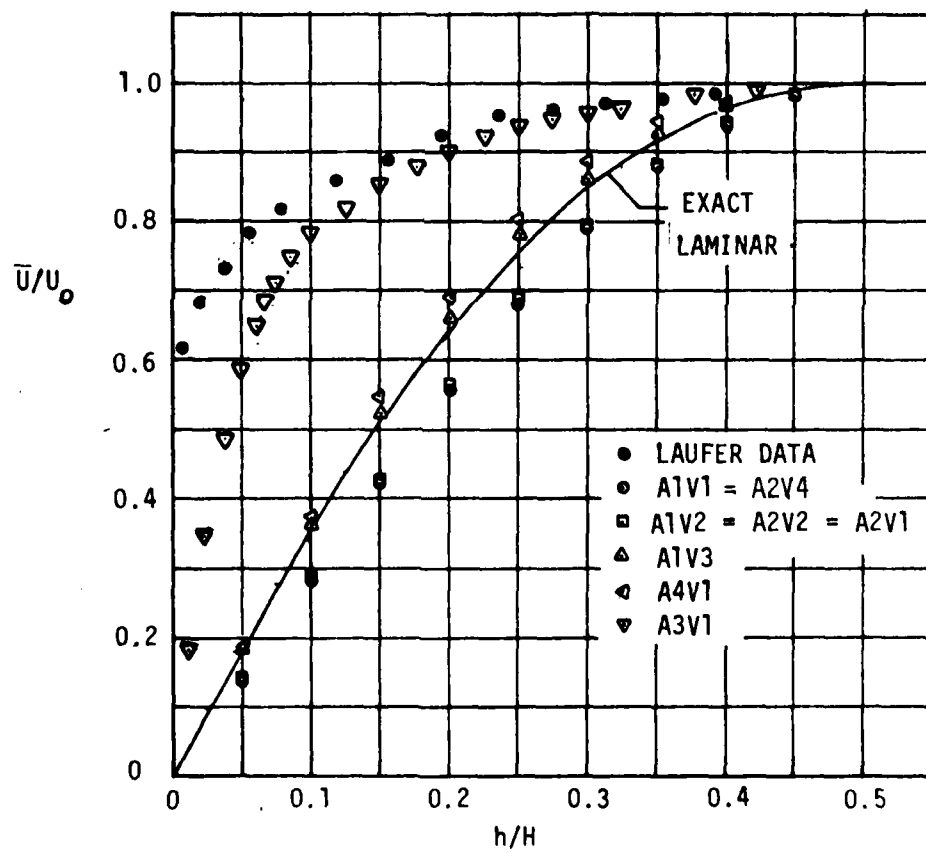
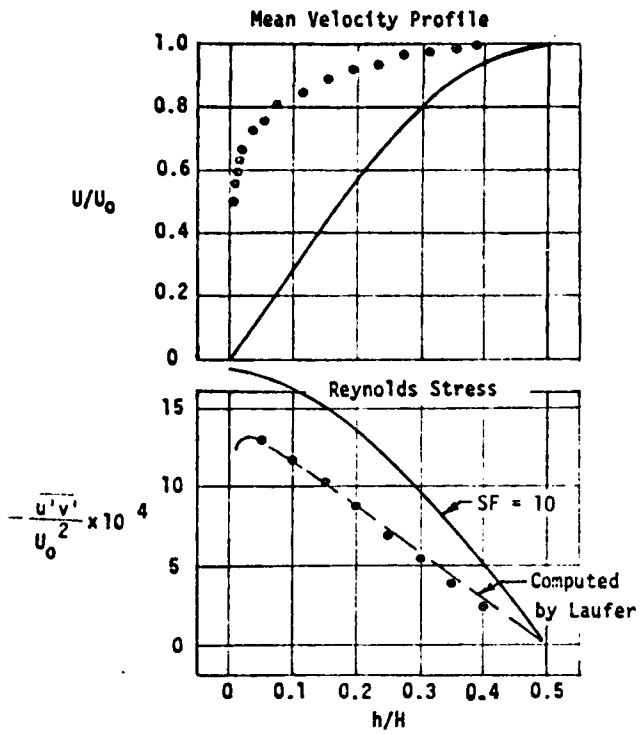


Figure 15. Mean Velocity Profiles Computed Using Arbitrary Vortex Distributions.



Data from Laufer, Reference (2)
Re = 30,800

SF = SCALE FACTOR
• Test Data
— Prediction

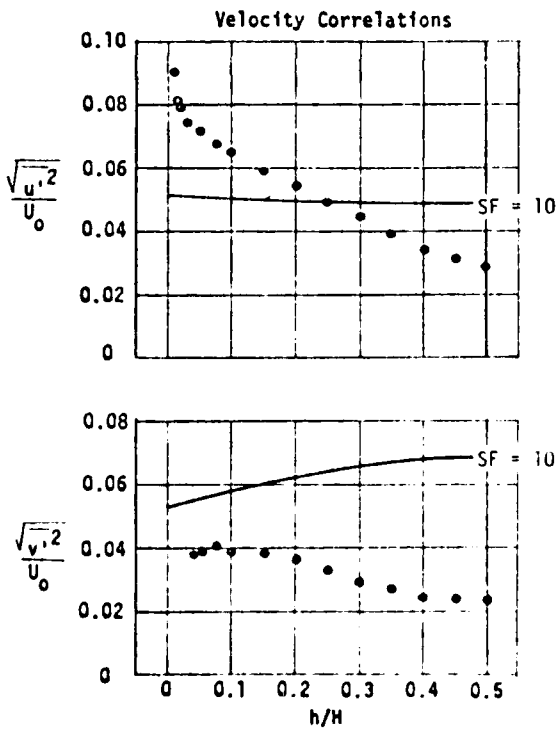
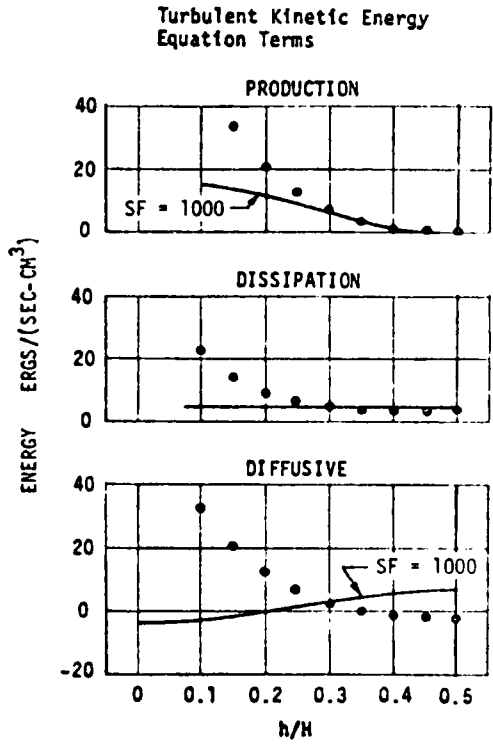
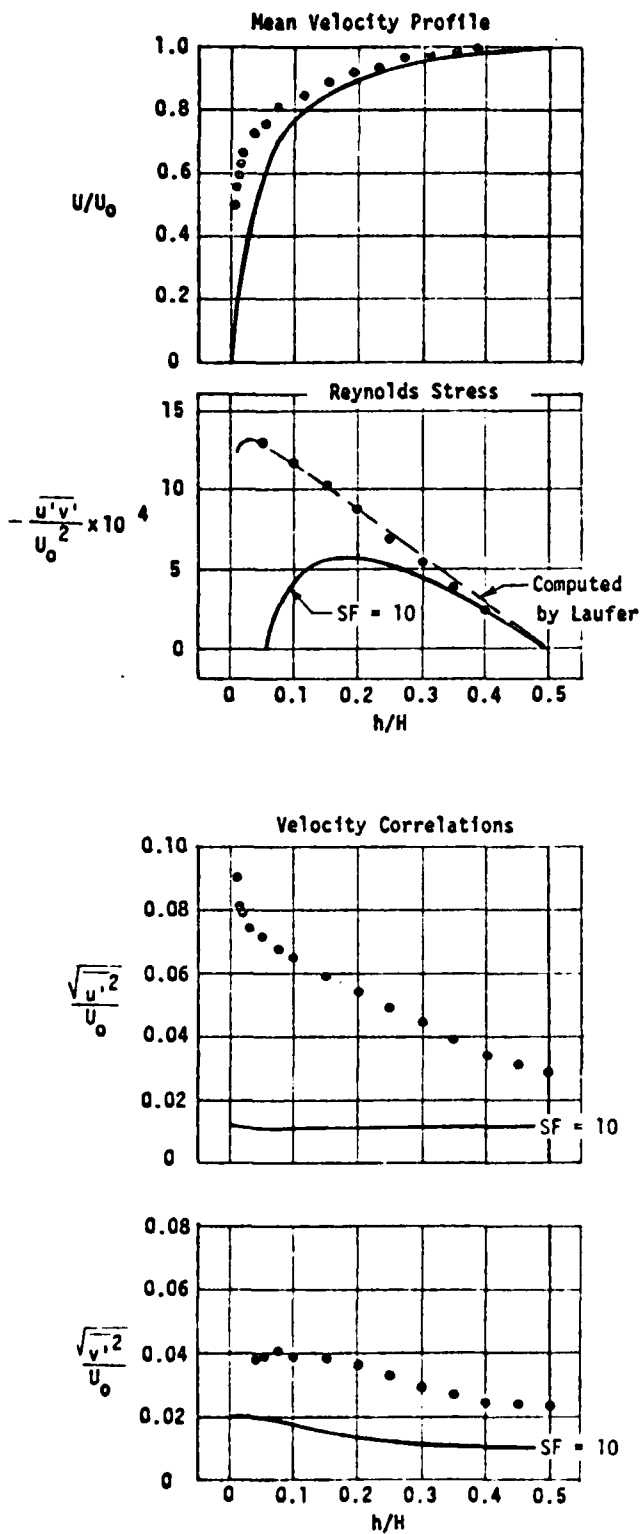


Figure 16. Comparisons of Data and Predictions with Distributions A2V4.



Data from Laufer, Reference (2)
 $Re = 30,800$

SF = SCALE FACTOR

• Test Data

— Prediction

Turbulent Kinetic Energy
 Equation Terms

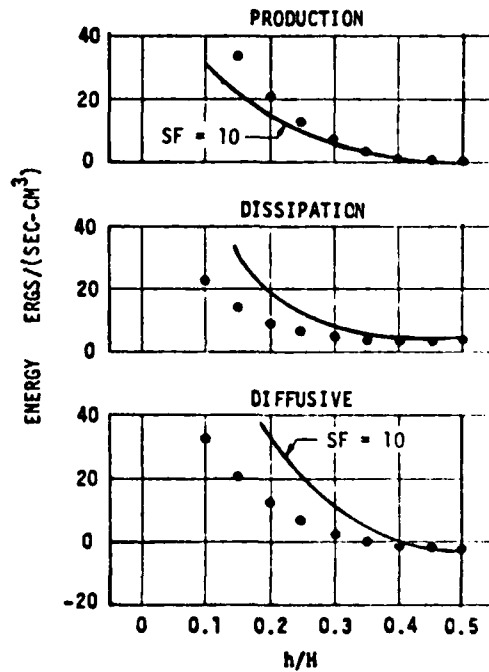


Figure 17. Comparisons of Data and Predictions with Distributions A3V1.

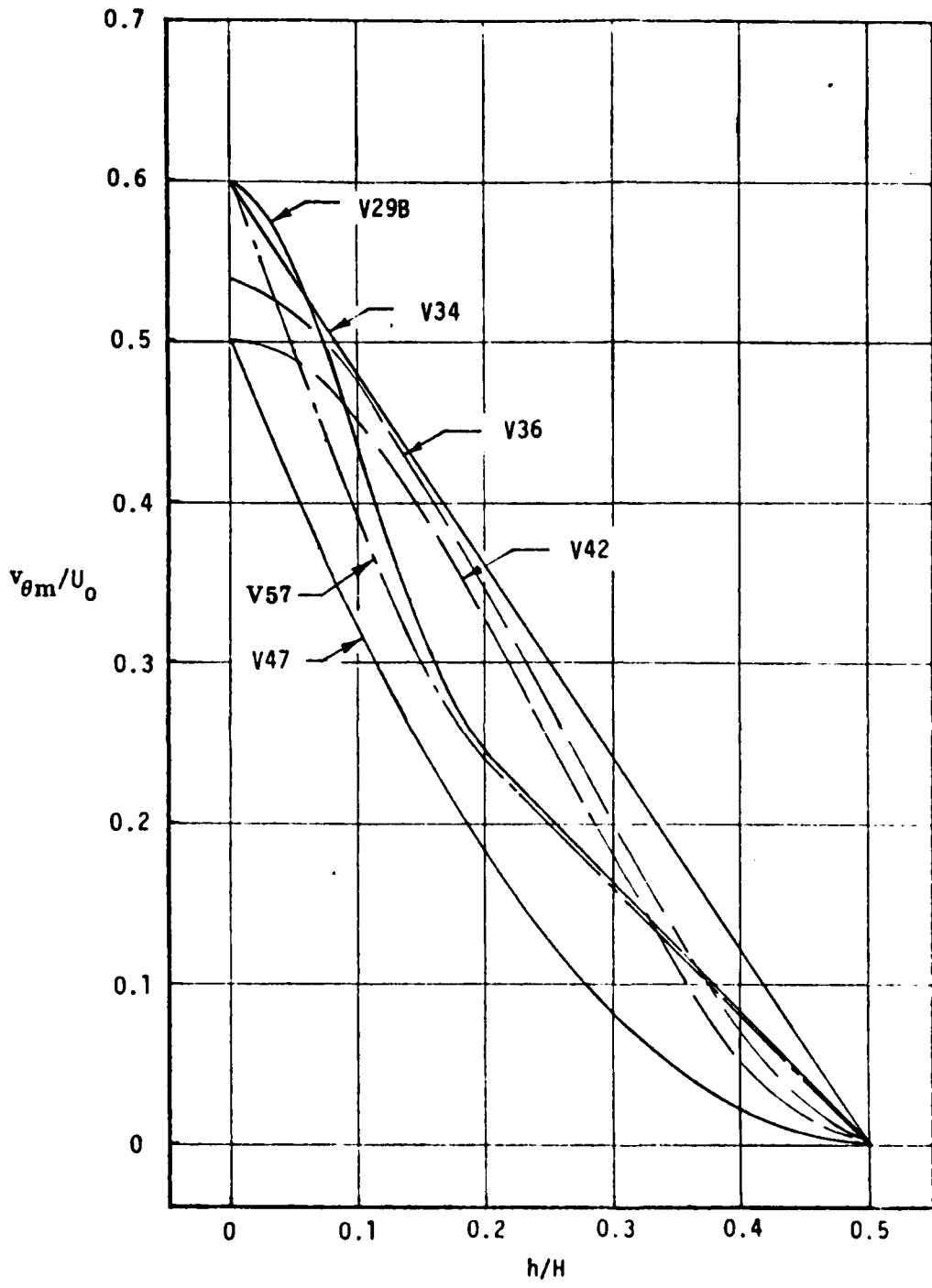


Figure 18(a). Vortex Strength Distributions

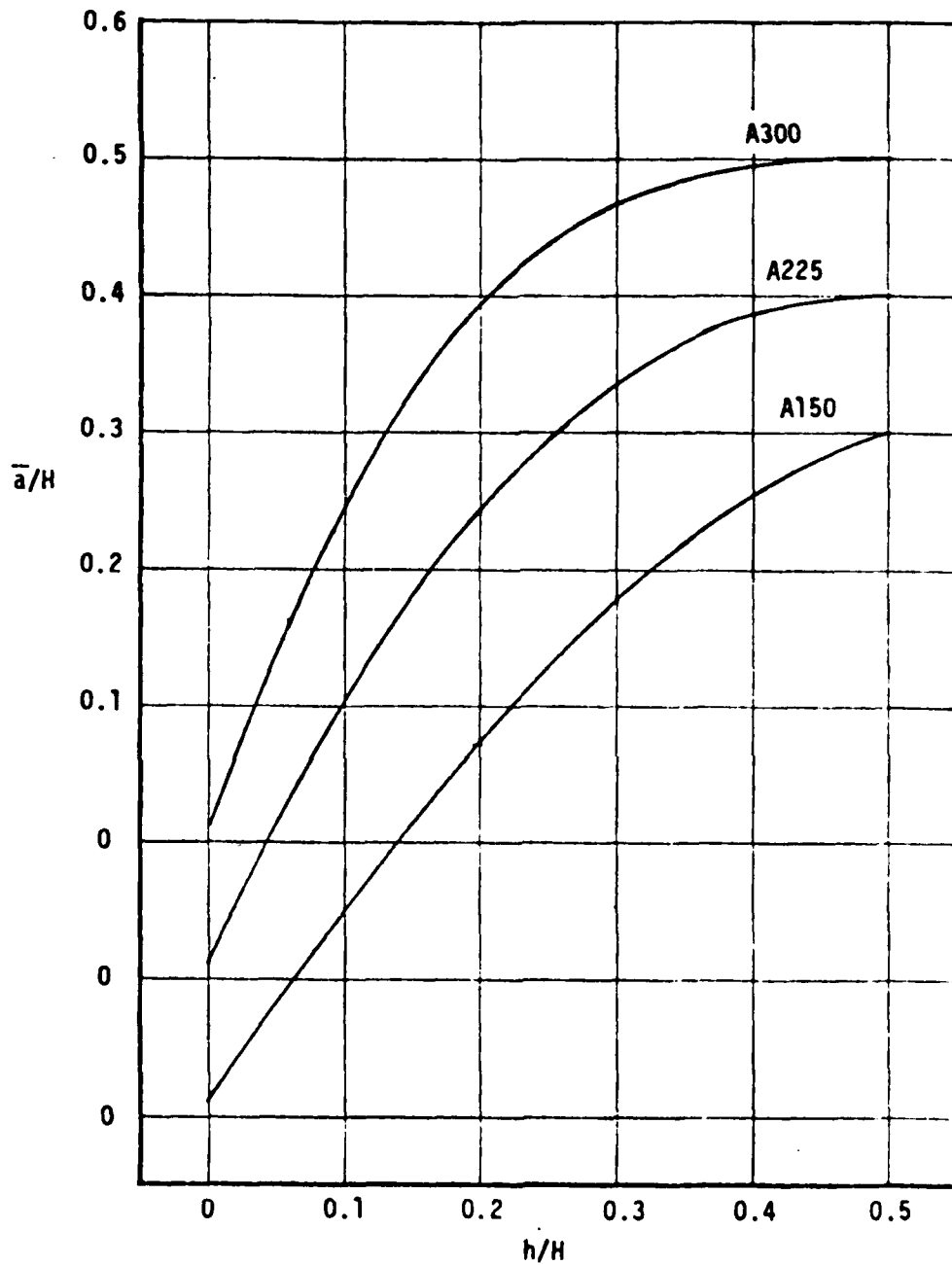


Figure 18(b). Vortex Size Distributions

The vortex size distribution affects the mean velocity profile and the Reynolds stress term. The mean velocity profile is sensitive to the initial slope (at the wall) of the vortex size distribution. This initial slope also affects the location of the peak value of Reynolds stress term. The level of the Reynolds stress term depends on the vortex size initial value (at the wall).

These observations are generally illustrated by the following comparisons, Figures 19 through 24. The predictions are compared to the $Re = 30,800$ flow case test data. Each figure corresponds to one of the vortex strength distributions of Figure 18(a) and includes the three vortex size distributions of Figure 18(b).

Mean Velocity Profiles

Note that the initial slope of the size distribution has a definite effect on the profile shape. The lower the initial slope, the fuller the profile. Vortex strength distribution V34, V36 and V42 yield the best match in terms of the mean velocity profile. The other vortex strength distributions yield profiles that are too full. This is characteristic of a higher Reynolds number flow; see Figure 13.

Reynolds Stress Term

The variation of Reynolds stresses computed using vortex strength distributions V34, V36 and V42 agree well with the data near the channel centerline but deviate the most towards the wall. Note that the peak values occur further from the wall. The initial slope of the vortex size distribution has a secondary but definite effect on the magnitude of the Reynolds stress.

Unsteady Velocity Correlations

The model now predicts the unsteady velocity correlation terms ($\overline{u'^2}$ and $\overline{v'^2}$) that are approximately equal to the test data. For the axial component ($\overline{u'^2}$), the predicted slope is generally lower than the test data. The vortex size variation with the lowest initial slope (A150) generally yields the best agreement. For the lateral component ($\overline{v'^2}$), the value near the centerline is well predicted, but tends to be high near the wall.

Turbulent Kinetic Energy (TKE) Terms

Vortex distributions V34, V36, and V42 yield the best comparisons for the production and dissipation terms. The diffusive term tends to be a little high. For the other vortex strength distributions, the production term tends to be slightly lower. In all these comparisons, the TKE terms increase rapidly as the wall is approached. This is due to the high turbulence levels near the wall. Laufer presented TKE levels only in the region away from the wall.

Summary

Vortex velocity distributions V36 and V42 give the best correlations with the test data. The mean velocity profile is well represented. The characteristic shape of the unsteady velocity fluctuations are also well characterized, as are the turbulent kinetic energy equation terms. The Reynolds stress distribution also correlates well near the duct centerline, but tends to deviate near the wall. Overall, the V29B/A300 distribution best matches the total data set.

The statistical vortex model of turbulence is based on the hypothesis that turbulence is composed of a series of vortices (eddies) with random properties which are convected downstream by the mean flow. The unsteady velocity correlations (and Reynolds stress term) are expressed in terms of the turbulence model vortex properties. These properties can be determined from measurements

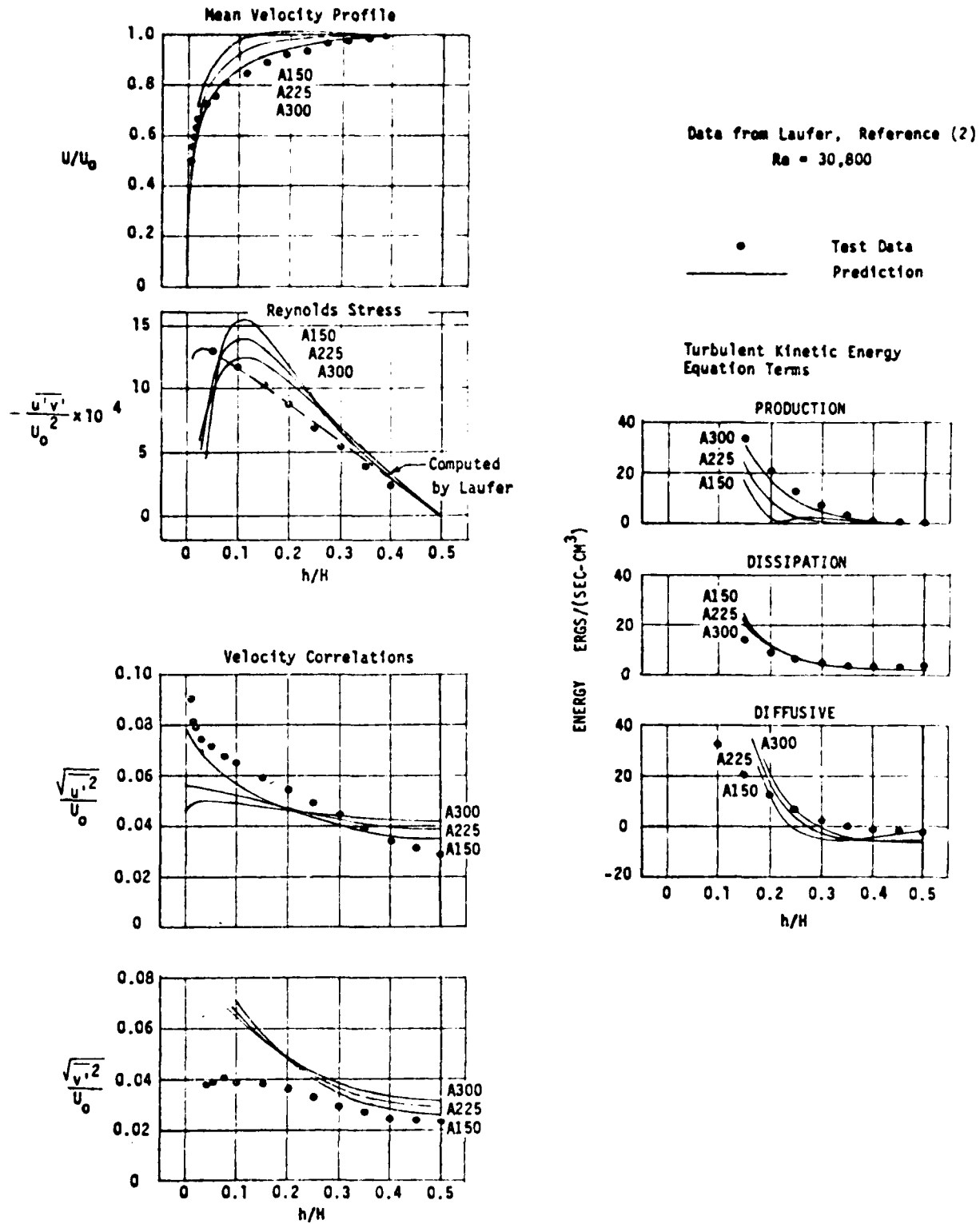
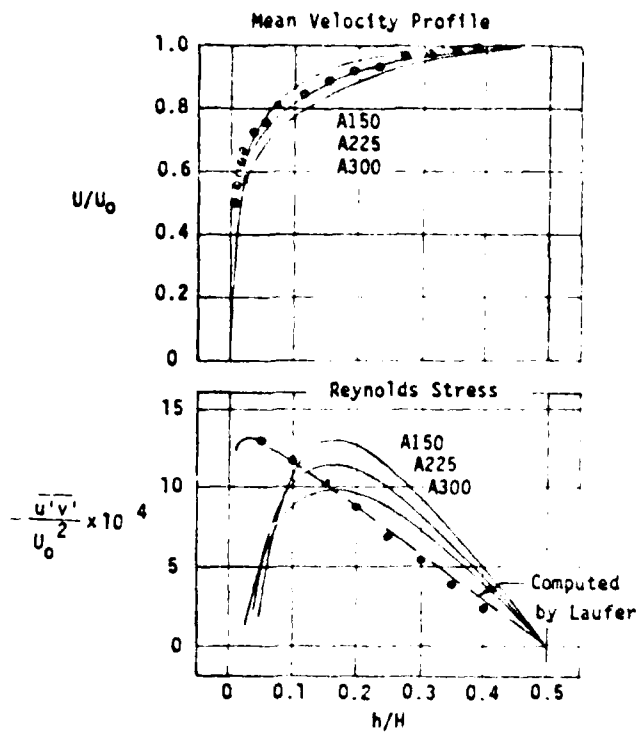


Figure 19. Comparisons of Data and Predictions with Distribution V298.



Data from Laufer, Reference (2)
 $Re = 30,800$

• Test Data
 — Prediction

Turbulent Kinetic Energy Equation Terms

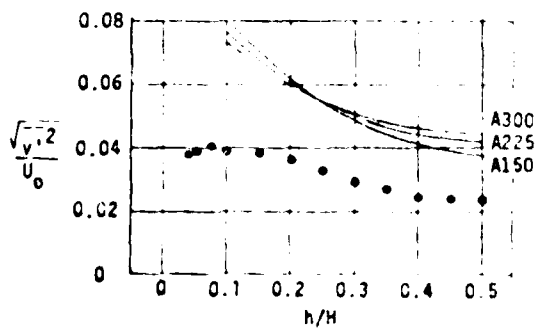
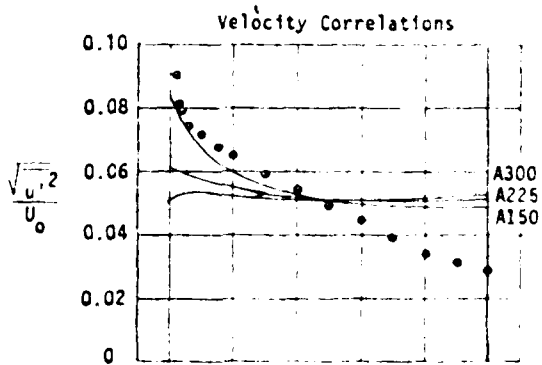
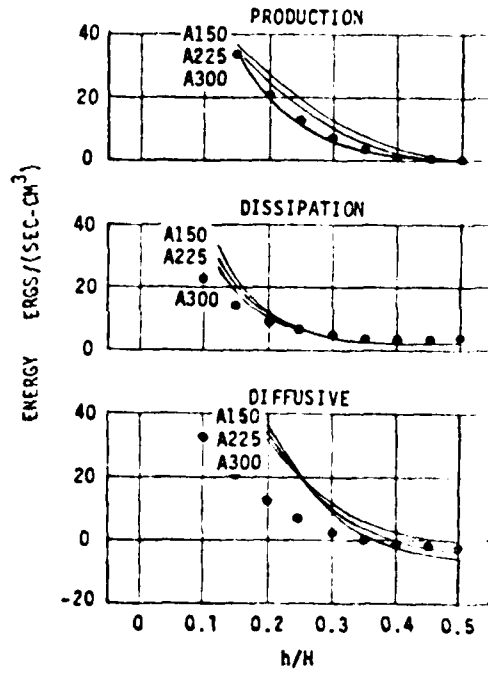
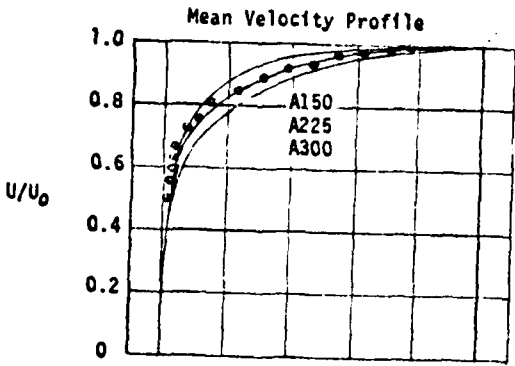
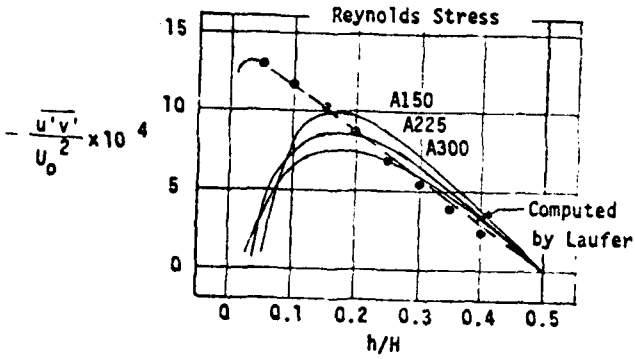


Figure 20. Comparisons of Data and Predictions with Distribution V34.



Data from Laufer, Reference (2)
Re = 30,800

• Test Data
— Prediction



Turbulent Kinetic Energy
Equation Terms

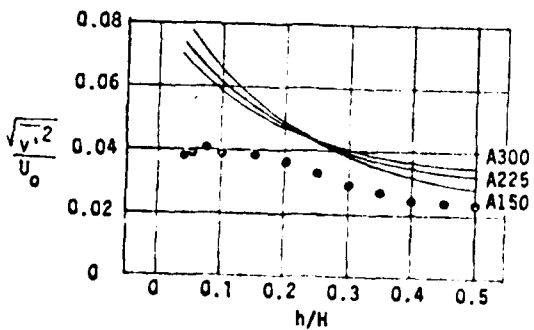
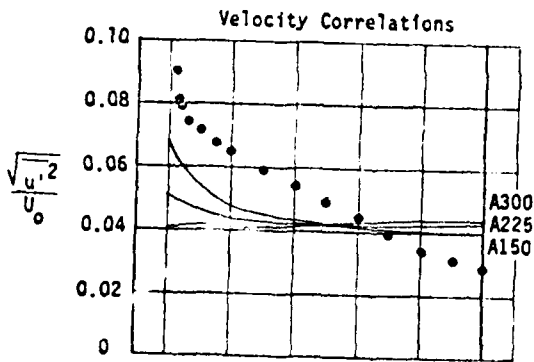
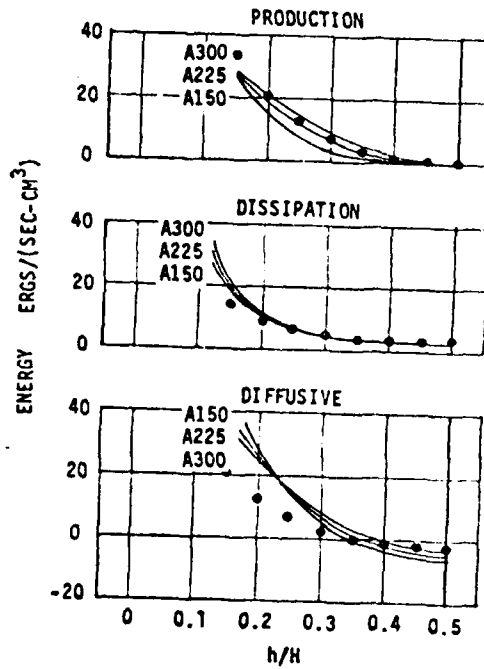
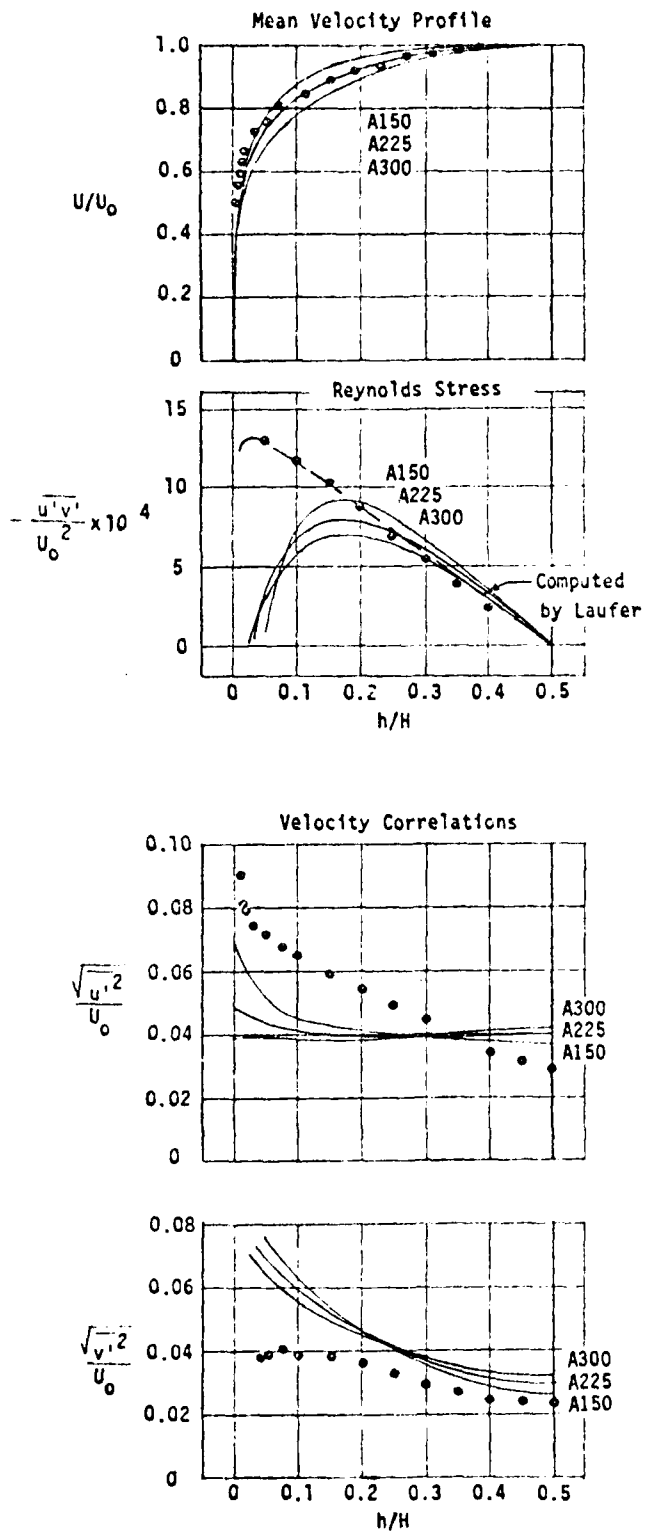


Figure 21. Comparisons of Data and Predictions with Distribution V36.



Data from Laufer, Reference (2)
Re = 30,800

• Test Data
— Prediction

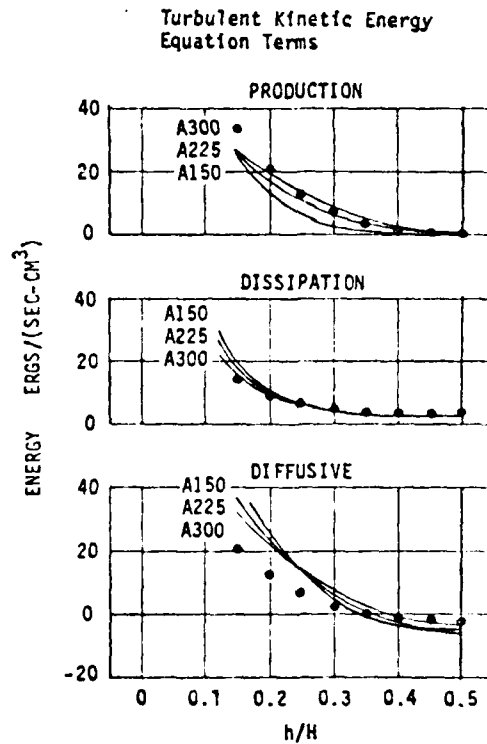
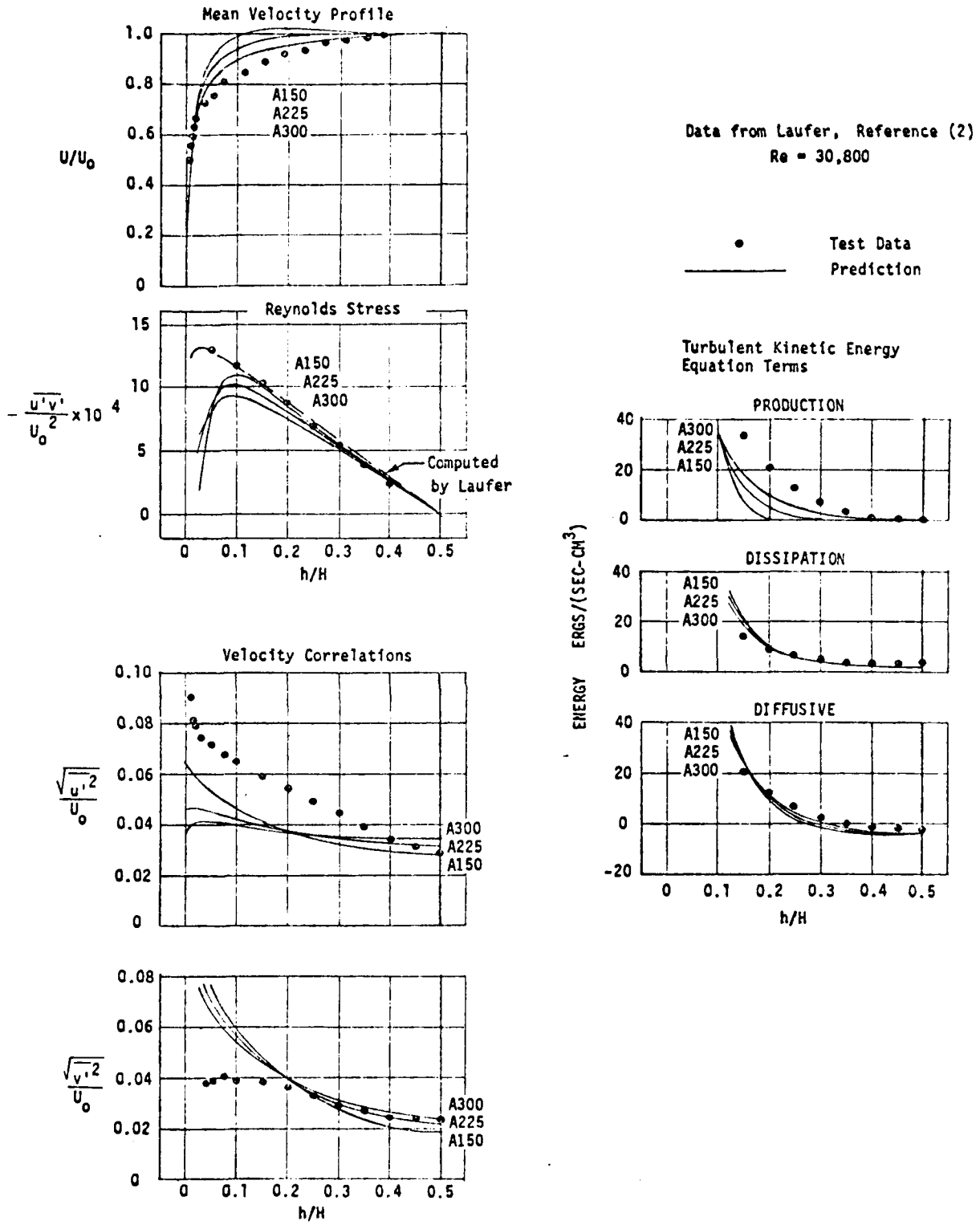


Figure 22. Comparisons of Data and Predictions with Distribution V42.



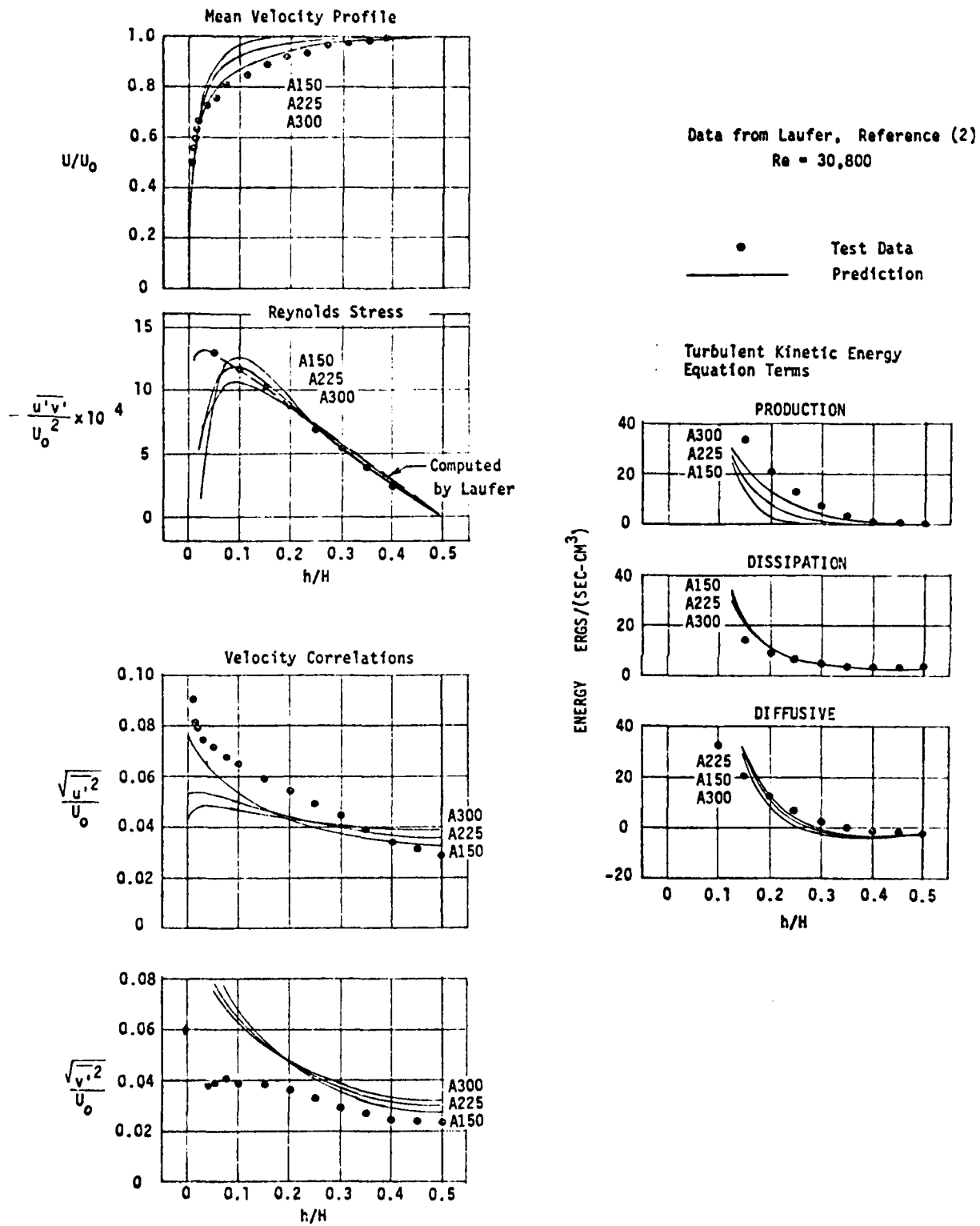


Figure 24. Comparisons of Data and Predictions with Distribution V57.

of the flow field unsteady pressure fluctuations. Since adequate measurements were unavailable, the vortex properties distributions were assumed and refined during the data/analysis comparisons to achieve agreement with the measure turbulence parameters.

Analytically, the statistical model of turbulence forms the closure required for the governing Reynolds and turbulent kinetic energy flow equations. The solutions obtained completely characterize the flow with a single distributive set of vortex (eddy) properties. Comparisons with a 2-D channel data base verified the characterizations.

2.6 ANALYSIS FOR AXISYMMETRIC FLOW AND JET MIXING

An outline is presented herein for extending the Turbulent Flow Model to the case of Axisymmetric Flow and Jet Mixing

2.6.1 Axisymmetric Flow

The flow field for fully developed turbulent flow in a duct of circular cross section is customarily described in cylindrical coordinates. The Reynolds Equation of Motion for this case is well established. The Turbulent Flow Model relations typified for the two-dimensional case are equally applicable to the axisymmetric flow case. The distributions of the vortex properties would be different, but these distributions can be established from measurements and/or comparisons with available data.

2.6.2 Jet Mixing

The jet mixing case is fundamentally a free shear flow field. This type of flow can be two-dimensional, axisymmetric, or of arbitrary shape. The Reynolds Equations of Motion for the 2-D and axisymmetric free shear flow are also well established. The Turbulent Flow Model must be adapted to this type of flow.

2.6.3 Outline of Procedure

The following steps are necessary to extend the procedure to axisymmetric flow and jet mixing:

- For Axisymmetric Flow Case:
 - o Assume axisymmetric flow
 - o Use cylindrical coordinate system
 - o Simplify Reynolds Equations of Motion
 - o Derive Turbulent Flow Model terms with
 - origin at centerline
 - zero velocity at wall/maximum at centerline
 - establish vortex property distributions
 - compare results to test data

- For Jet Mixing:
 - o Assume axisymmetric flow
 - o Use Reynolds Equations derived above
 - o Adapt Turbulent Flow Model terms for
 - maximum velocity core flow region
 - changing (expanding) boundary
 - freestream velocity beyond boundary
 - verify with test data

3.0 CONCLUSIONS AND RECOMMENDATIONS

The feasibility study to solve the Reynolds Equations of Motion for fully developed turbulent flow in a two-dimensional channel has led to the following conclusions:

- The turbulent flow model provides a means for obtaining closure for the governing Reynolds Equations of Motion and Turbulent Kinetic Energy Equation.
- The turbulent flow model yields a direct solution of the mean velocity profile.
- The turbulent flow model yields the distribution of the Reynolds stress across the channel to solve the Reynolds Equations.
- The turbulent flow model also yields good agreement in the axial and lateral unsteady velocity correlation terms.
- The turbulent flow model yields good agreement for the production, dissipation, and diffusive terms of the turbulent kinetic energy equation.

The agreement in all these aspects of the turbulent flow using a single distribution set of vortex or eddy functions confirm the applicability of the Turbulent Flow Model to the solution of the general turbulent shear flow problem. Therefore, it is highly recommended that the overall program of Jet Scaling be continued. The next phase is to extend the analytical techniques to the case of axisymmetric flow and jet flow.

REFERENCES

1. Melick, H. C., "Analysis of Inlet Flow Distortion and Turbulence Effects on Compressor Stability," NASA CR114577, 31 March 1973.
2. Laufer, John, "Investigation of Turbulent Flow in a Two-Dimensional Channel," NACA Technical Report 1053, 1951.
3. Prandtl, L. and Tietjens, P. G., Applied Hydro and Aeromechanics, Dover Publications, Inc., 1975.
4. Roshko, Anatol, "Structure of Turbulent Shear Flows: A New Look," AIAA Paper No. 76-78 (Dryden Lecture) presented at 14th Aerospace Sciences Meeting, Washington, D. C., January 26-28, 1976.
5. Hinze, J. O., Turbulence, McGraw-Hill Book Company, New York, 1959.
6. Shampine, L. F. and Gordon, M. K., Computer Solution of Ordinary Differential Equations, W. H. Freeman and Co., 1975.
7. Townsend, A. A., The Structure of Turbulent Shear Flow, Second Edition, Cambridge University Press, 1976, p. 136.

NOMENCLATURE

A1, A2, etc.	- vortex size distribution labels
a	- vortex core size, see Figure 6
B	- vortex model vorticity constant, Equation (14)
c_s	- vortex flux spacing constant, see Table III, $c_s = 1.845$
d	- vortex lateral spacing, see Table III
e	- 2.71828
f()	- function of
H	- two-dimensional channel height
Hz	- Hertz
ℓ	- vortex axial spacing, see Table III
N	- vortex flux rate, see Table III
n	- vortex spin direction, see Table I
P, p	- pressure
PSD	- power spectral density function
P()	- probability of ()
q	- dynamic pressure
q	- resultant velocity, $q^2 = u^2 + v^2$
r	- vortex radius, $r = a$ at maximum velocity
Re, Reo	- Reynolds number
RMS	- root-mean-square value
SF	- scale factor, see Figures 16 and 17
t	- time
TKE	- turbulent kinetic energy
U, V	- absolute velocity in axial (X) and lateral (Y) direction
u, v	- unsteady velocity components in axial (X) and lateral (Y) direction

NOMENCLATURE (Continued)

$\overline{u'^2}, \overline{v'^2}$	- unsteady velocity correlation terms
$\overline{u'v'}$	- Reynolds stress term
$V_1, V_2, \text{ etc.}$	- vortex strength distribution labels
V_θ	- vortex tangential velocity
X, Y	- axial and lateral direction coordinates

Greek Symbols

Δ	- increment or change
θ	- vortex tangential direction
μ	- absolute viscosity
ν	- kinematic viscosity
π	- 3.14159
ρ	- density

Subscripts

i	- individual vortex
m	- maximum value
o	- based on channel maximum velocity
w	- at the wall
θ	- in vortex tangential direction